ĒL

(FOUO)

3 APRIL 1979

FOR OFFICIAL USE ONLY

JPRS L/8366

3 April 1979

SELECTED ARTICLES

FROM THE JOURNAL 'QUANTUM ELECTRONICS'

USSR

U. S. JOINT PUBLICATIONS RESEARCH SERVICE

FOR OFFICIAL USE ONLY

NOTE

JPRS publications contain information primarily from foreign
newspapers, periodicals and books, but also from news agency
transmissions and broadcasts. Materials from foreign-language
sources are translated; those from English-language sources
are transcribed or reprinted, with the original phrasing and
other characteristics retained.

Headlines, editorial reports, and material enclosed in brackets
[] are supplied by JPRS. Processing indicators such as [Text]
or [Excerpt] in the first line of each item, or following the
last line of a brief, indicate how the original information was
processed. Where no processing indicator is given, the infor-
mation was summarized or extracted.

Unfamiliar names rendered phonetically or transliterated are
enclosed in parentheses. Words or names preceded by a ques-
tion mark and enclosed in parentheses were not clear in the
original but have been supplied as appropriate in context.
Other unattributed parenthetical notes within the body of an
item originate with the source. Times within items are as
given by source.

The contents of this publication in no way represent the poli-
cies, views or attitudes of the U.S. Government.

FOR OFFICIAL USE ONLY

SELECTED ARTICLES

FROM THE JOURNAL 'QUANTUM ELECTRONICS'

<div align="center">

CONTENTS   PAGE

</div>

<div align="center">

- a -   [I - USSR - L FOUO]

</div>

FOR OFFICIAL USE ONLY

FOR OFFICIAL USE ONLY

CONTENTS (Continued)   Page

FOR OFFICIAL USE ONLY

FOR OFFICIAL USE ONLY

PUBLICATION DATA

English title   : SELECTED ARTICLES FROM JOURNAL
                                    'QUANTUM ELECTRONICS'

Russian title   : KVANTOVAYA ELEKTRONIKA

Author (s)   :

Editor (s)   : N.G. Basov

Publishing House   : Sovetskoye radio

Place of Publication   : Moscow

Date of Publication   : 1978

Signed to press   :

Copies   :

COPYRIGHT   : Izdatel'stvo "Sovetskoye radio",
                                    "Kvantovaya elektronika", 1978

- c -

HIGH-SPEED WIDE-BAND ELECTROOPTICAL LITHIUM NIOBATE ELEMENTS FOR LASER BEAM CONTROL SYSTEMS

[Text] A study is made of the frequency and pulse charac-
teristics of modulators and polarization switches of digi-
tal deflectors made of 0°-cut lithium niobate crystals.
Methods are proposed for increasing the operating range of
these devices by correcting the electric control signals.
A single-stage switching time on the order of 300 nanosec-
onds was obtained.

It is also presented from experimental studies of the frequency and pulse
characteristics of electrooptical devices made of 0°-cut lithium niobate
crystals. The possible methods   llarging the passband and increasing
the speed of these devices are investigated.

Let us consider the factors determining the nature of the frequency-ampli-
tude characteristic of an electrooptical crystal. As is known, the linear
electrooptical effect is possible in ferroelectric crystals in which a pi-
ezoelectric effect is also observed. On application of a controlling elec-
tric field to this crystal, deformations occur which lead to variation of
the refraction coefficients. Thus, a "secondary" effect is imposed on the
"true" electrooptical effect caused by the inverse piezoelectric and opto-
elastic effects.

The variation of the polarization constants Δa_{ij} of the nondeformed optical
index in a mechanically free crystal can be described as follows for the ex-
istence of both effects [1]:

$$\Delta a_{ij} = r^T_{ijk} E_k = (r^s_{ijk} + p_{ijlm} d_{klm}) E_k,\qquad(1)$$

where r^T_{ijk} are the total effect coefficients; r^s_{ijk} are the coefficients of
the true electrooptical effect; p_{ijlm} are the optoelastic coefficients of

1

FOR OFFICIAL USE ONLY

the crystal; E_k are the controlling field components; d_{klm} are the piezo-
electric moduli.

In a mechanically squeezed crystal the electrooptical effect is determined
only by the coefficient r^8.

The conditions of mechanical squeezing in the crystal are also realized when
controlling a fast-alternating field as a result of the inertia of the pi-
ezoelectric effect inasmuch as the inertia of the "true" electrooptical ef-
fect is several orders smaller. Thus, the level of the frequency-amplitude
characteristic of the crystal is distinguished within low-frequency and high-
frequency bands of the controlled frequencies. The effectiveness of the de-
vices made of the $0°$-cut lithium niobate based on using the coefficient r_{22}
at high frequencies diminishes by almost two times.

The ultrasonic waves propagated in the crystal experience reflection from
its boundaries, and on coincidence of an integral number of half-wavelengths
with the geometric size of the sample in the direction of propagation, me-
chanical resonance occurs. The resonance frequencies $f_{p_{in}}$ of the rectangu-
lar resonator are defined by the expression

$$f_{p_{in}} = \frac{n v_i}{2 d_i}, \quad i = x, y, z \tag{2}$$

where n are the integral numbers defining the order of the overtone; d_i is
the size of the sample with respect to the direction of the wave propaga-
tion; v_i are the elastic wave velocities in the crystal. In addition, reso-
nance is also possible on combination frequencies of the basic tones and
harmonics.

In the resonance range, the contribution of the secondary electrooptical ef-
fect varies significantly, which defines the significant nonlinearity of the
frequency-amplitude characteristic of the element (the values of the total
electrooptical coefficients with respect to range can differ by several
times). The Q-factor of the system decreases with an increase in frequency;
the high-order overtones are weakly exhibited, and the total electrooptical
coefficient decreases to a value of r^8, which corresponds to the squeezed
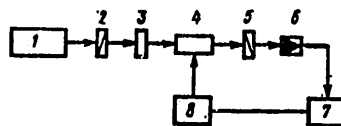crystal.

Figure 1. Diagram of the experimental setup for recording the modulation
coefficient and the half-wave voltage as a function of frequency:
1--laser; 2--polarizer; 3--$\lambda/4$ plate; 4--investigated sample; 5--
analyzer; 6--photoreceiver; 7--Khl-27 frequency-amplitude charac-
teristic meter (oscillograph); 8--submodulator (SF-28 oscillator).

2

FOR OFFICIAL USE ONLY

We have investigated the frequency characteristics of the electrooptical elements made of $0°$-cut lithium niobate with the application of a controlling field along the X-axis of the crystal by two methods.

The frequency-amplitude characteristics were recorded by the first method for a small controlling voltage with an amplitude of 0.1 $U_{\lambda/2}$ ($U_{\lambda/2}$ is the half-wave voltage). The diagram of the device for taking the measurements is presented in Figure 1. The Khl-27 frequency characteristic meter and wide-band amplifier (submodulator) were used in the setup. The accuracy of this method is low, for the joint frequency-amplitude characteristic of the crystal and the photoreceiver is measured, but the method does permit simple, fast determination of the frequency-amplitude characteristics of the elements in a wide frequency range. It is also necessary to note that the controlling electrooptical element is a nonlinear device and, consequently, the shape of the frequency-amplitude characteristic does not sufficiently accurately characterize the sample even for an ideal receiver, for it depends strongly on the amplitude of the controlling signal and the bias for a nonlinear device.

The frequency-amplitude characteristics of elements made of lithium niobate of various geometric sizes were recorded. Figure 2 shows one such characteristic for a sample with dimensions of $x = 4.3$ mm, $y = 6.5$ mm and $z = 16$ mm. It is obvious that the first resonance frequency is in the 400-kilohertz range. On application of the controlling field along the X-axis for samples with dimensions along the Y and Z axes commensurate with the dimension along the X-axis, the shape of the frequency-amplitude characteristic of the element depends little on these dimensions, that is, the dimension along the direction of the applied field is defining.

The relation for the primary resonance frequency as a function of the dimensions along the X-axis is presented in Figure 3 in accordance with the experimental results. These results agree well with the values of the resonance frequencies that were calculated for the ultrasonic wave velocities in lithium niobate and were presented in [2].

Thus, it is obvious that the modulating element made of $0°$-cut lithium niobate can be used either in the low control frequency range (to frequencies of several hundreds of kilohertz) or the use of a carrier frequency in the high-frequency range (the lower bound of the range--tens of megahertz).

However, many electrooptical devices must have modulation bands from zero to tens of megahertz with low nonuniformity, or they must have a frequency-amplitude characteristic of a form such as to permit correction as a result of the control system (for the frequency-amplitude characteristic of the free sample depicted in Figure 2, this is impossible).

The known methods of broadening the band consisting either in decreasing the size of the elements, that is, in carrying the resonance frequencies beyond the operating range [3], or consisting in squeezing the crystal [4, 5], are

3

not always applicable. In the former case, the crystal aperture is decreased significantly (see Figure 3). In the latter case, the optical quality of the crystal is foiled, and the orthogonal component of the light field (background) appears at the output of the device in the absence of a control voltage. In addition, it has not been possible to damp the crystal fully (see the frequency-amplitude characteristic of a sample with massive electrodes, Figure 2).
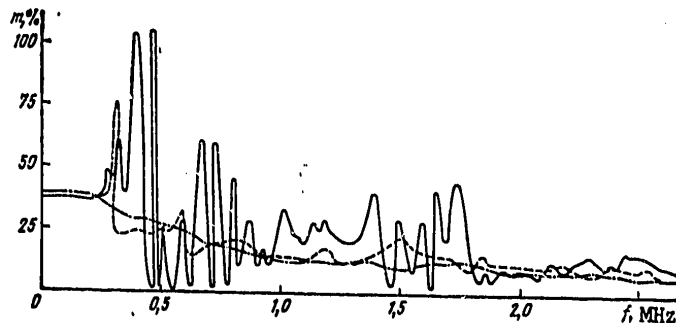
Figure 2. Frequency-amplitude characteristics of a lithium niobate sample: solid curve--free sample; dashed curve--sample with massive silver electrodes; dash-dot curve--sample with nonreflecting faces.
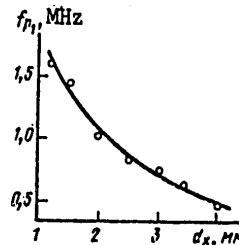
Figure 3. First resonance frequency as a function of the sample size d_x.

We have proposed and used a method of eliminating resonances as a result of the fact that at the boundary of the electrooptical element conditions were created under which reflection of the ultrasonic waves does not occur. They are taken out of the crystal and are scattered outside it. The frequency-amplitude characteristic of the controlling element with nonreflecting faces is also presented in Figure 2. The optical quality of the sample in this case is almost no worse.

A similar electrooptical element made of lithium niobate with dimensions of x = 1.5 mm, y = 2 mm and z = 20 mm was used in the modulator of a device for recording information by a laser beam. The dynamic values of the half-wave voltage were used as an exact characteristic of the frequency properties of

4

the sample. As is known [6], the modulation characteristic of the system made up of the electrooptical element and the analyzer with sinusoidal controlling signal and using quarter-wave bias has the form

$$I = I_0 \sin^2\left[\frac{\pi}{2}\frac{U_0 \sin \omega t}{U_{\lambda/2(\omega)}} + \frac{\pi}{4}\right], \tag{3}$$

where I is the light intensity of the output; I_0 is the maximum light intensity at the output; U_0 is the amplitude of the controlling signal with a frequency ω.

The measurements of the magnitude of the half-wave voltage were performed on a device, the optical part of which is analogous to that presented in Figure 1. The controlling voltage with amplitude U_0 was fed from the GS-28 oscillator on fixed frequencies directly to the tested sample. From the photoreceiver the signal went to the y-plates of the oscillograph, and for scanning the controlling signal $U_0 \sin \omega t$ was used. The modulation characteristic defined by the expression (3) was observed on the screen of the oscillograph. On varying U_0 and reaching the maximum of the signal I, it is possible to determine the half-wave voltage on the given frequency by the formula

$$U_{\lambda/2}(\omega) = 2U_0. \tag{4}$$

This method determining the frequency characteristic is more exact by comparison with the first method, for the shape of the frequency characteristic is fixed, and the frequency-amplitude characteristic of the photoreceiver does not influence the measurement error.
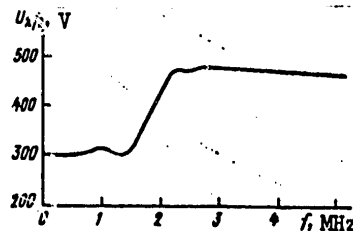
Figure 4. Half-wave voltage as a function of frequency for a sample with nonreflecting faces.

The values obtained for the half-wave voltage are presented in Figure 4. It is quite obvious that the suppression of the resonances is effective, and on high frequencies the contribution of the secondary electrooptical effect disappears, as a result of which the half-wave voltage increases. The transition from the low-frequency to the high-frequency region has a monotonic nature, and the steep drop of the frequency-amplitude characteristic of the electrooptical element can be compensated in the high-frequency range by correction of the controlling voltage with respect to the known law by

ordinary radio engineering methods. In the mentioned modulator this was done by simple high-frequency correction of the frequency-amplitude characteristic of the submodulator. The modulator passband of 0-2.5 megahertz was obtained with ±10 percent nonuniformity. It is also possible to obtain significantly larger modulation bands by complicating the correction of the preliminary electronic amplifiers.

The contrast of the modulator exceeded 100, that is, the proposed method of eliminating resonances in practice had no negative effect on the optical quality of the crystal. Thus, this method combined with correction of the controlling signal permits the creation of wide-band (from zero to tens of megahertz) electrooptical modulators with good optical quality and high linearity of the frequency-amplitude characteristic without reducing the transverse cross section of the crystal. The analogous modulators can find application in wide-band communication lines, high-speed shutters and other such devices.

Along with the modulators, the most important class of electrooptical devices includes the digital electrooptical deflectors [6], which are a series of successively arranged binary cells (stages) made up of an electrooptical polarization switch and a splitting element.

Let us consider what determines the speed of this type of deflector. The modulation characteristic of one stage is given by the expression (3), and the intensity of the output signal of the deflector with simultaneous commutation of the N stages is proportional to $\sin^{2N}$ of the feed voltage.

This permits determination of the required voltage level γ_N with respect to the given level I/I_0 at the output of the deflector on switching N stages:

$$\gamma_N = \frac{2}{\pi} \arcsin \sqrt[2N]{\frac{I}{I_0}}. \qquad (5)$$

Thus, for example, for N = 12 and a light intensity level at the output of 0.9 of the static value, a voltage level on the stages of 0.945 of the half-wave value ($\gamma_{12} = 0.945$) is required.

Here it is also necessary to consider the following facts: the frequency-amplitude characteristic of the element has a steep drop in the mechanical squeezing region (see Figure 4), and the controlling element is essentially nonlinear.

The frequency-amplitude characteristic of an electrooptical element (see Figure 3) can be represented by the expression

$$K(j\omega) = K_1 + K_2/(1 + j\omega\tau), \qquad (6)$$

where τ is the time constant; K_1, K_2 are the coefficients taking into account the contribution of the primary and secondary electrooptical effects.

6
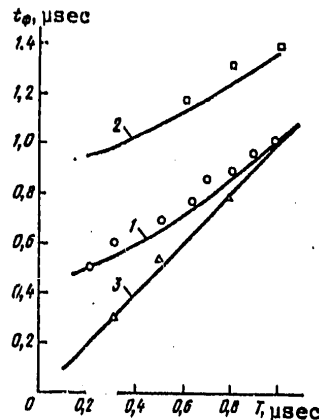
Figure 5. Calculated time for buildup of the light intensity to the 0.9
level as a function of the controlling pulse front duration:
1--single stage; 2--12-stage deflector; 3--single stage with cor-
rected controlling pulse. The points near the curves are the ex-
perimental data.

For the $0°$-cut lithium niobate on application of the controlling field along
the X-axis, $K_1 \approx 0.6$ and $K_2 \approx 0.4$. The second term of the expression (6)
takes into account the contribution of the secondary electrooptical effect
and is approximated by a function of the transmission coefficient of the
low-frequency filter.

On feeding a controlling pulse of the single-step type with linearly in-
creasing front of duration T to the electrooptical element characterized by
the transfer function (6), the light signal at the output can be determined,
using, for example, the operation method [7] as follows. The image of the
acting signal has the form

$$U(j\omega) = \frac{1}{T(j\omega)^2}(1 - e^{-j\omega T}). \tag{7}$$

Multiplying (7) by the transfer coefficient (6), we obtain the image of the
reaction. On going to the original, we find the light signal in the form

$$\frac{I_{max}}{I_0} = \sin^{2N}\frac{\pi}{2}\left\{\frac{t}{T}\sigma(t) - \frac{t-T}{T}\sigma(t-T) - K_2\frac{\tau}{T}[(1-e^{-t/\tau})\sigma(t) - \right.$$
$$\left. - (1 - e^{-(t-T)/\tau})\sigma(t-T)]\right\}, \tag{8}$$

where $\sigma(t)$ is a unique discontinuity.

Setting the relative voltage level equal to γ_{12}, from (8) we obtain the
light pulse front duration at the output of the 12-stage deflector:

7

$$t_\phi \cdots \tau \ln \frac{(K_2\tau/T)|\exp{(T/\tau)} - 1|}{1 - \gamma_0}. \tag{9}$$

Figure 5 shows the relations for the setup time of the light response with respect to the 0.9 level for one stage and for a 12-stage deflector as a function of the front duration of the controlling electric pulse calculated according to (9) and also values obtained experimentally. It is obvious that for the given crystal aperture, it is impossible to obtain a deflector speed less than 0.8 microseconds by a simple shortening of the controlling pulse front.

The time constant τ determining the speed of the element can be decreased by decreasing the dimensions of the crystal, but this leads to a decrease in the aperture and, consequently, the number of deflected positions.

Another means of increasing the speed reduces to varying the shape of the controlling signal in order to emphasize the high frequencies in its spectrum so as to compensate for the steep drop of the frequency-amplitude characteristic of the element in the high-frequency range. This can be achieved by creating a blip on the controlling signal front.

Let, for example, a pulse of the following type be superposed on the signal with linearly increasing front T

$$U(t) = \alpha[\sigma(t - T) \cdots \sigma(t - T - \Delta)], \tag{10}$$

where α is the relative amplitude of the pulse; Δ is its duration. Using the above-described procedure [7], let us define the light signal at the output of the controlling element with the transfer coefficient defined by the expression (6) for $t \geq T + \Delta$:

$$I(t)/I_0 = \sin^2\frac{\Pi}{2} \{1 - (K_2\tau/T)(e^{T/\tau} - 1)e^{-t/\tau} + K_2\alpha[e^{\Delta/\tau} - 1]e^{-(t - T)/\tau}\}. \tag{11}$$

This expression is exactly equal to one under the condition

$$(\tau/T)(e^{T/\tau} - 1) \approx \alpha(e^{\Delta/\tau} - 1)e^{T/\tau}, \tag{12}$$

permitting determination of the ratio between α and Δ for the given T and τ.

This method of increasing the speed was checked experimentally. The controlling pulse had a special form with a blip in the initial section. As a result of this correction, the switching time of one stage was reduced to 300 nanoseconds for small distortions of the peak.

Figure 6 shows the oscillograms of the controlling and the light pulses with and without correction. It is obvious that the correction significantly shortens the light pulse fronts.

8

FOR OFFICIAL USE ONLY
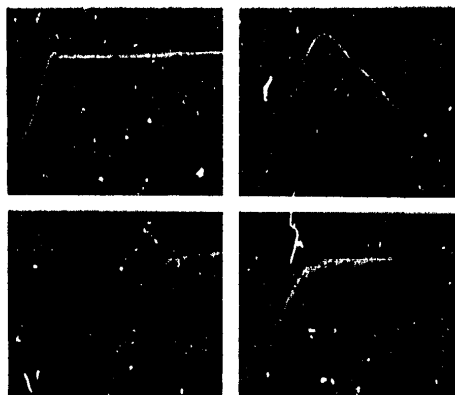
Figure 6. Oscillograms of the controlling pulses (a, b) and the light pulses (c, d). The oscillogram c corresponds to the controlling pulse a. The oscillogram d corresponds to the controlling pulse b. The scale is as follows: 100 nanoseconds/division.
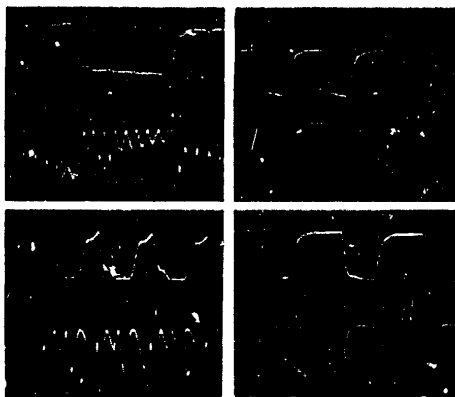
Figure 7. Oscillograms of pulses obtained with undamped (a, b) and damped (c, d) crystals. The upper beams are the controlling electric signals; the lower beams are the light response. Scale: 2 microseconds/division.

Further shortening of the fronts is possible by increasing the blip amplitude and giving it a defined shape. The difficulties arising in this case are connected with the selection of the shape of the blip which determines the distortions of the flat peak of the light pulse. In order to obtain

9

FOR OFFICIAL USE ONLY

FOR OFFICIAL USE ONLY

maximum speed and low distortions of the peak, the blip must be asymmetric with small buildup time and comparatively gentle decrease (about 500 nano-seconds for given crystal size along the X-axis).

The output light pulses of the electrooptical deflectors can be significantly distorted also as a result of the resonance properties of the electrooptical element. The separation of the spectral components of the control signal takes place on comparison of their frequencies with the characteristic fre-quencies of the crystal, and it is exhibited in the modulation at the peak of the pulse and in the pulse interval. The admissible degree of distor-tions can be realized by limiting the spectrum of the controlling signal which is equivalent to decreasing the speed or by operation of the deflectors on fixed frequencies which narrows the area of their application.

The distortions of the light pulse peaks can be decreased to admissible val-ues by damping the crystals using the above-mentioned method proposed by us. In this case the magnitude of the distortions in practice does not depend on the period and the duration of the controlling pulses, and it is determined by the steepness of their fronts. Figure 7 shows the oscillograms of light pulses in the case of undamped and damped crystals for various combinations of periods and durations of the controlling pulses. The shape of the light signal switched by the damped crystal in practice does not depend on the op-erating conditions.

The results show that a combination of damping with correction of the shape of the controlling signal permits at the present time realization of a 14-stage electrooptical deflector (4,096 positions) with less than 15-percent distortion of the pulses under the worst conditions (simultaneous commuta-tion of all stages) for a switching time on the order of 0.7-0.8 microsec-onds.

In conclusion, the authors express their appreciation to V. S. Smorodinov and N. V. Kartashev for the developed and delivered control units permitting the experiment to be performed.

BIBLIOGRAPHY

1. J. Nay, "Fizicheskiye svoystva kristallov i ikh opisaniye pri pomoshchi tenzorov i matrits" [Physical Properties of Crystals and Their Descrip-tion Using Tensors and Matrices], Moscow, Mir, 1967.

2. Ye. Zh. Spenser, P. V. Lenzo and A. A. Bolmen, TIIER, Vol 55, No 12, 1967, p 5.

3. R. P. Riesz and M. R. Blazz, APPL. OPTICS, No 8, 1969, p 1393.

4. T. Mitoki, PRIBORY DLYA NAUCHNYKH ISSLEDOVANIY, No 3, 1972, p 165.

FOR OFFICIAL USE ONLY

FOR OFFICIAL USE ONLY

5. C. D. Butter, T. C. Lee and J. D. Look, "Proc. of the Technical Program 'Electrooptical Systems Conference, 1972,'" N. Y., 1972, p 171.

6. Ye. R. Mustel' and V. N. Parygin, "Metody modulyatsii i skanirovaniya sveta" [Methods of Light Modulation and Scanning], Moscow, Nauka, 1970.

7. M. A. Lavrent'yev and B. V. Shabat, "Metody teorii funktsiy kompleksnogo peremennogo" [Methods of the Theory of Functions of a Complex Variable], Moscow, Nauka, 1973.

10845
CSO: 8144/0821-22

11

FOR OFFICIAL USE ONLY

FOR OFFICIAL USE ONLY

USE OF EXCITED ATOMS IN THERMALLY INITIATED VISIBLE CHEMICAL LASERS

[Article by A. S. Bashkin, N. L. Kupriyanov and A. N. Orayevskiy, Physics
Institute imeni P. N. Lebedev of the USSR Academy of Sciences, Moscow; sub-
mitted 20 June 1977, revised 22 September 1977]

[Text] An analysis is made of the possibility of obtain-
ing continuous (quasicontinuous) generation in the ultra-
violet and visible regions with pumping in a chemical re-
action with the participation of excited atoms. The re-
action takes place during the mixing of fluxes of excited
atoms and the corresponding reagent. The excited atoms
(first excited state) are formed on recombination of a
plasma during the fast cooling process in a supersonic
nozzle. Specific reactions are proposed. The theoreti-
cal possibility of obtaining generation by this system on
XeF and HgCl molecules is demonstrated.

1. Recently a great deal of attention has been given to the creation of
visible chemical lasers based on electron transitions of molecules formed in
chemical reactions. The reactions of the particles in the ground electron
state are successfully used in infrared chemical lasers (for example, on HF
and CO molecules) but for the electron transitions the intense searches for
generation in the reactions of this type still have not led to success [1,
2].

The studies of the dynamics of bimolecular exchange reactions indicate that
the reactions of the electron-excited particles in the majority of cases
will permit us to obtain electron-excited molecules with high quantum yields.
For example, the quantum yield in the reactions of the excited atoms of noble
gases with a number of fluorine-containing compounds is close to one [3].
Recently there have been reactions of formation of electron-excited mole-
cules from excited Hg atoms [4, 5], Cd atoms [4], and atoms of the alkali
metals Rb, Cs [6]. The initiation of the reactions by an electron beam made
it possible to obtain generation on the electron transitions of XeF, KrF and
other molecules [1]. Here the excited atoms of the inert gases are formed

12

FOR OFFICIAL USE ONLY

on passage of fast electrons through a dense gas. Although the electron-excited molecules are formed in the chemical reaction here, the basic energy is still extracted from the pumping source.

Accordingly, it is unquestionably of interest to study the feasibility of obtaining continuous generation in such reactions with the participation of excited atoms formed by the thermal method (if the heating of the gas takes place as a result of the chemical energy, this laser will be purely chemical). In the case investigated by us, the reaction takes place with mixing of the fluxes of the reagents (just as in the traditional chemical continuous lasers [15]), one of which contains excited atoms. The thermal method of the formation of excited atoms consists in using two different mechanisms: plasma and atomic recombination. These mechanisms correspond to two types of internal energy of the heated gas connected with the transition of the particles to the continuous spectral states, that is, ionization and dissociation.

Plasma Mechanism. In this case the atoms in the excited states are formed as a result of electron-ion recombination on cooling of a thermally ionized gas in a supersonic nozzle. The joint effect of the collision and radiation relaxation leads to predominant population of the first excited state which relaxes the essentially slower upper state [7]. If this state is radiation-connected to the ground state, then the capture of the resonance radiation can ensure an increase in the effective lifetime. The difference in the proposed system from the principles of plasma-dynamic lasers developed in [7] consists in using the most populated first excited level. Its population was investigated previously as a harmful process of loss of excitation.

The parameters of a thermally ionized gas, depending on the temperature, follow from the Saha equation

$$n_e n_i / n_a = K_e(T) \equiv (g_i g_e / g_a)(2\pi m_e k' T / h^2)^{3/2} \exp(-E_i / k' T),$$

where k' is the Boltzmann constant. The values of the equilibrium density of the electrons are presented in the table for temperatures of $10^{4\circ}$ K and $5 \cdot 10^{3\circ}$ K and gas density of $n_a = 10^{18}$ cm^{-3} for certain atoms, indicating the possibilities of the thermal method of creating a plasma. The plasma with parameters close to the presented ones can be obtained using plasmotrons, shock waves and high-temperature flames.

Element	n_e, cm^{-3}		E_i, eV
	$T = 10\,000$ K	$T = 5\,000$ K	
Kr	$5.5 \cdot 10^{16}$	$3 \cdot 10^{13}$	14
Xe	$1.7 \cdot 10^{17}$	10^{14}	12,1
Hg	$2.5 \cdot 10^{17}$	$3.5 \cdot 10^{14}$	10,44
Cd	10^{18}	$2.7 \cdot 10^{15}$	9
Na	10^{18}	$7 \cdot 10^{16}$	5,14
Cs	10^{18}	$3 \cdot 10^{17}$	3,9

Atomic Recombination Mechanism. This mechanism consists in the formation of excited atoms in the process of recombination of atomic particles with the participation of three bodies. Its general scheme can be represented as follows:

$$R + Q + A \rightarrow RQ + A^*,$$
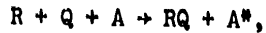
where R and Q are the recombining atoms or radicals; A^* is the excited atom. The energy of excitation of the atoms A is theoretically limited to the energy of the R-Q bond and it can reach a value of ~ 9 electron-volts for the recombination reactions of C+O, N+N. A most complete study is made of these processes under the conditions of excitation of additives of Tl, Pb, Cd and Zn metals to the different flames [8]. Another example is the reaction [10]

$$O + O + O \rightarrow O_2 + O(^1S).$$
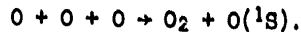
The advantage of this mechanism is the lower initial gas temperature, for as a result of high statistical weight of the continuous states, the majority of gases are sufficiently dissociated at temperatures of $\sim 3,000-4,000^\circ$ K. As the calculations show, the internal energy of the gas under such conditions primarily consists of the free recombination energy, which promotes the achievement of high efficiency.

2. For analysis of the specific reactions and operating molecules it is necessary primarily to obtain an expression for the amplification coefficient and the inversion condition in general form. The possibility of this approach arises from the presence of general features both for the excited atom reactions and for electron transitions of lasing molecules.

We shall consider that the fluxes containing excited A^* atoms are mixed with the accompanying fluxes of the BC reagents. Then the chemical reaction of the formation of electron-excited AB^* molecules will take place in the mixing zone:

$$A^* + BC \rightarrow AB^* + C. \tag{1}$$

It is advantageous to place the axis of the resonator perpendicular to the planes of the fluxes. This "transverse" system is preferable in the case of a high reaction rate, such as, for example, in the continuous HF chemical lasers [15].

Now let us consider the ratio of the characteristic times of different processes in order to select an appropriate calculation technique. Let k^* be the rate constant of the reaction (1) with the formation of the electron-excited AB^* molecule, let k be the total rate constant of the reaction (1) for all states of the products (as has already been noted, we shall consider the reactions for which $k^*/k \approx 1$). If the concentration [BC] > [A^*], then the characteristic time of occurrence of the chemical reaction is determined by the expression $\tau_x = (k[BC])^{-1}$. The reactions of the excited atoms are

14

characterized by high rate constants (weakly dependent on the temperature) $\sim 10^{-10}$ cm^3/sec. The minimum concentration of the reagents is determined by the condition of achievement of threshold inversion on the electron transition in the visible region and, probably, cannot be less than 10^{15} cm^3/sec. Thus, $\tau_x < 10^{-5}$ sec.

The decay of the excited AB* molecules is possible along two channels--collision and radiation:

$$AB^* + M \xrightarrow{k_1} B + AM(M^*), \tag{2}$$

$$AB^* \xrightarrow{\tau_{rad}^{-1}} B + A h\nu. \tag{3}$$
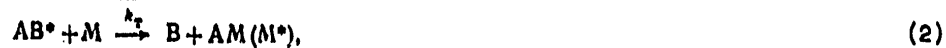
Let us introduce the characteristic decay time τ_p of the excited AB* molecule by the expression $1/\tau_p = (k_T[M])^{-1} + 1/\tau_{rad}$. For determinacy we shall consider that the electron transition (3) is resolved so that $\tau_p < 10^{-6}$ sec. This condition corresponds to the majority of known systems and in any case does not increase the final result.

In addition, let us define the mixing time τ_π as $\tau_\pi = a/u$, where a is the length of the mixing zone of the fluxes; u is their velocity. Experience in creating continuous chemical lasers permits us to set $\tau_\pi \geq 10^{-5}$ sec (a > 1 cm, u $\sim 10^{-5}$ cm/sec).

Thus, the investigated model is characterized by the following expression of the characteristic process times:

$$\tau_\pi > \tau_x > \tau_p. \tag{4}$$

The smallness of the decay time of the excited state by comparison with the mixing time and the reaction time makes it possible to consider the concentration of excited molecules quasistationary and to calculate it by the formula

$$[AB^*] = [A^*][BC]k^*\tau_p. \tag{5}$$

The conditions (4) also indicate that when calculating the amplification coefficient it is necessary to consider the final mixing rate of the reagents. For this purpose we shall use the model of the flame front which is used successfully to calculate HF continuous chemical lasers [10] and permits determination of the concentrations of the reagents averaged across the flux and the gas-dynamic parameters. The advantage of this model is connected with the fact that in order to calculate laser systems the average values of the concentrations are needed. For determinacy let us set [BC] > [A*] (which permits us to neglect the BC flow rate), and let us consider the flow to be isothermal and to occur in a channel of constant cross section. Then the equation for the concentration average to cross the flow can be written in the form

FOR OFFICIAL USE ONLY

$$\frac{d}{dx} \langle y_f(x) | A^* | \rangle = |A^*|_0 \frac{dy_f(x)}{dx} - \frac{\langle y_f(x) | A^* | \rangle}{l_x},$$ (6)

where $y_f(x)$ is the width of the flame front as a function of the coordinate along the flux x; $[A^*]_0$ is the initial concentration of A^*, and l_x is the characteristic length corresponding to the time τ_x and defined by the expression $l_x = u/(k[BC])$. The various mixing mechanisms (laminar, turbulent) are taken into account in the expression for the function $y_f(x)$. Here we shall limit ourselves to the case of turbulent mixing where [11]

$$y_f(x) = \begin{cases} hx/l_D, & x < l_D, \\ h, & x \geqslant l_D, \end{cases}$$

h is the width of the fluxes; l_D is the characteristic mixing length (l_D = 10h [11]). Then the solution to equation (6) with zero initial condition is determined by the expression

$$\langle y_f(x)[A^*] \rangle = h[A^*]_0 (l_x/l_D)[1 - \exp(-x/l_x)]$$ (7)

for $x < l_D$.

Postponing the investigation of the inversion condition for the time being and considering that it is satisfied, let us write the expression for amplification across q fluxes:

$$\chi = q\sigma \langle [AB^*] y_f(x) \rangle.$$

Here σ is the induced radiation cross section of the investigated electron transition from the lower vibrational level of state of AB^* (fast vibrational relaxation of the state is assumed). Let us convert this formula considering (5) and (7):

$$\chi = q\sigma\tau_p [A^*]_0 \frac{k^*}{k} \frac{uh}{l_D} \left[1 - \exp\left(\frac{-x}{l_x}\right)\right].$$

The maximum amplification is reached for $x = l_D$, and since the condition (4) can be rewritten in the form $l_D > l_x$, the expression for χ_{max} is simplified:

$$\chi_{max} \approx q\sigma\tau_p [A^*]_0 \frac{k^*}{k} \cdot \frac{u}{10}.$$ (8)

It is necessary to note that in the used model the amount of amplification does not depend on the pumping reaction rate constant or on the concentration of the second component which is connected with the form of expression (5) and the proposition of turbulent mixing. The formula obtained makes it possible to determine the order of magnitude of characteristic concentration of the excited atoms required to set aside the self-excitation condition. Let us illustrate this in the following example: threshold amplification equal to 0.1, $u = 10^5$ cm/sec, $\sigma = 10^{-16}$ cm^2 and $\tau_p = 10^{-6}$ sec (characteristic

16
FOR OFFICIAL USE ONLY

values for the resolved electron transitions) and a number of layers q = 100, it is necessary to have $[A^*]_0 = 10^{15}$ cm^{-3}.

3. Up to now we have neglected the population of the lower laser level. However, the accumulation of molecules in the ground electron state can lead to fast disruption of the inversion and, consequently, to ineffective use of the excited atoms. The problem of depopulation of the lower laser levels must be solved considering the peculiarities of the specific molecules. However, in the investigated model it is possible to take out the general condition which the various mechanisms of the relaxation of the lower levels must satisfy.

After the flame front the overall concentration of the reaction products (1) is equal to $[A^*]_0$ (under the condition that the thickness of the positive amplification layer is much less than the width of the mixing zone, for $l_x \ll l_D$). Then the light absorption on the frequency of the operating transition by the reaction products in the mixing zone will be

$$a(x) = \sigma \langle y_\Gamma(x)[AB'] \rangle = \sigma[A^*]_0 y_\Gamma(x) F(x),$$

where [AB'] is the concentration of the AB molecules on the lower laser level, and F(x) is defined by the expression $F(x) = [AB']/([AB] + [B])$, and it is a function of the distribution of the AB molecules in the ground electron state considering their dissociation. If the dissociation of the AB molecules does not take place, then F(x) coincides with the vibrational-rotational distribution function, for [B] = 0. This introduction of F(x) permits us to consider the molecules with low dissociation energy (for example, XeF) at high temperatures. Now let us write out the condition that the amplification exceeds the absorption for total use of the A* atoms (considering (8)):

$$a/\chi = hF(l_D)/(\tau_p u) < 1. \tag{9}$$

This condition must be satisfied for any type of distribution function. If the vibrational equilibrium cannot be established, then F(x) depends on the vibrational relaxation rate. However, in the case of fast establishment of equilibrium with respect to vibrational levels of the ground electron state and the dissociation equilibrium (fast by comparison with the time τ_π determining the length of the reaction zone), the distribution function F(x) depends only on the aggressive temperature at the flux point x. The investigation of the equilibrium case is also of interest from the point of view of determining the maximum gas temperature in the active region for which the positive amplifications still exist.

The equilibrium constant of the reaction AB $\rightleftharpoons$ A + B can be represented in the form $K = K_0 \exp(-D/kT)$, where K_0 is the factor which depends weakly on the temperature, and D is the dissociation energy [18]. Hence, we obtain the expression for F:

17

FOR OFFICIAL USE ONLY

$$F = \frac{[1 - \exp(-\omega''/k'T)] \exp(-E_0 \cdot /k'T) [A]}{K_0 \exp(-D/k'T) \cdot \mathbf{i} \cdot [A]}$$ (10)

ω'', v'' are the vibrational quantum and the number of the lower electron state, respectively. The condition $hF(1_D)/(\tau_p u) = 1$ jointly with (10) can be considered now as the equation for determining the maximum temperature of existence of positive amplification in the mixing zone. The formulas obtained make it possible to estimate the required flux parameters of the excited atoms and the other BC reagent in each specific case.

4. In this paper we shall limit ourselves to the analysis of the flame mechanism of formation of excited atoms. Let us consider the peculiarities of the kinetics of the recombining plasma determining the population of the first excited state so that the feasibility of this procedure will be qualitatively explained. We are interested in the decay of the equilibrium plasma with a temperature of $T \gtrsim 10^{4\circ}$ K and an electron concentration of $n_e \gtrsim 10^{15}$ (as follows from expression (8) for concentration of the excited atoms).

The population of the first excited state A^* takes place as a result of the joint occurrence of the recombination processes and subsequent relaxation of the highly excited levels. The latter process takes place quite rapidly [7, 18]; therefore it is possible to use the approach of the stationary discharge for the highly excited states. Then the pumping of the state A^* is defined by variation of the degree of ionization $|d\alpha/dt|$. In contrast to the highly excited levels, A^* reacts significantly more slowly. In the case of an optically dense plasma (or metastable A^*) its decay takes place during collisions with the electrons and atoms. The corresponding rate constants k_T^e and k_T^a have characteristic values of 10^{-10} cm^3/sec and 10^{-14} cm^3/sec, and they depend weakly on the temperature [18]. Thus, with an increase in the electron concentration, both the pumping intensity and the quenching rate increase, which leads to the existence of optimal initial parameters of the plasma for which the concentration $[A^*]$ after cooling is maximal.

Let us define these parameters. In order to avoid the numerical solution of the problem of the flow of a relaxing gas in a nozzle, let us use a model of the inertial separation which is used successfully to explain the qualitative peculiarities [7]. Then the dependence of the total particle concentration on time can be written in the form $n = n_0(t_0/t)^\mu$. Here μ is the dimensionality of the problem (for a wedge-type nozzle $\mu = 1 - 2$); $t_0 = H/2u$, where H is the width of the critical cross section; u is the flux velocity; the time is reckoned from the time t_0.

Let us write the equation for the "degree of excitation" $\varepsilon = [A^*]/n$ taking into account the above-enumerated processes:

$$\frac{d\varepsilon}{dt} = \left| \frac{d\alpha}{dt} \right| - (k_T^e n\alpha + k_T^a n) \varepsilon.$$ (11)

18

FOR OFFICIAL USE ONLY

In order to find ε it is necessary to define the dependence of the degree of ionization α on time. At the time t_0 the equilibrium degree of ionization α is defined by the Saha formula. In the initial stage of expansion α can be traced after the temperature and $\alpha = \alpha_p(T)$. Then the temperature decreases so much that the ionization process is "switched off," the rate of which is proportional to the small factor $\exp(-E_i/k'T)$. The variation of the degree of ionization is now determined wholly by recombination; therefore the kinetic equation for α can be written in the form

$$d\alpha/dt = -k_p n^2 \alpha^3, \qquad\qquad (12)$$

where k_p is the rate constant of the three-particle recombination ($k_p \sim T^{-3/2}$).

We shall consider that the replacement of the equilibrium ionization regime by the kinetic one takes place instantaneously at the time t_1 determined from the equality $k_p(t_1)n_e^2(t_1) = [(2T_1/E_1)t_0]^{-1}$ [18] (the characteristic recombination time is equal to the time of variation of the electron density as a result of cooling). Let us also propose that the electron temperature is equal to the gas temperature and satisfies the expression $(T/T_0)^{1/(\gamma-1)} = n/n_0$ with $\gamma = 5/3$ (the adiabatic expansion). This is valid for a low degree of ionization when it is possible to neglect the heat release as a result of recombination. In addition, the realization of the regime of interest to us with accumulation of the excited atoms also decreases the heat release. For example, for Xe this approach is valid for $\alpha < 40$ percent. Omitting the intermediate calculations, let us write the expression for α:

$$\alpha = \begin{cases} \alpha_0 \exp\left\{-\dfrac{E_i}{2T_0}\left[\left(\dfrac{t}{t_0}\right)^{u(\gamma-1)} - 1\right]\right\} & \text{for } t_0 < t < t_1, \\[2em] \dfrac{\alpha_1}{\left\{1 + \dfrac{2k_p(t_1)n_e^2(t_1)t_0}{\mu+1}\left[\left(\dfrac{t}{t_1}\right)^{\mu+1} - 1\right]\right\}^{1/2}} & \text{for } t > t_1. \end{cases}$$

For $t > t_1$, the solution to equation (12) is written with the initial condition $\alpha = \alpha_1$. The general solution of equation (11) has the form

$$\varepsilon(t) = \left\{\int_{t_0}^{t} dt'' \left|\frac{d\alpha}{dt}\right| \exp\left[\int_{t_0}^{t''} (k_r^i n\alpha + nk_r^a)\, dt'\right]\right\} \exp\left[-\int_{t_0}^{t} (k_r^i n\alpha + nk_r^a)\, dt'\right].$$

Here we have neglected the initial value of $\varepsilon(t_0)$ by comparison with α_0.

The factor $\exp[-I(t)]$ (where $I(t) = \int_{t_0}^{t}(k_r^i n\alpha + nk_r^a)\,dt'$) is the fraction of the atoms decaying in the cooling process at the time t. The region of convergence of the integral $I(t)$ is several units of t_0. Consequently, for a degree of cooling $T/T_0 \sim 0.1$ it is possible to use the value of $I(\infty)$. It is obvious that the satisfaction of the inequality $I(\infty) < 1$ is sufficient for

quenching the first excited state where $\varepsilon(\infty) \approx \alpha_0$, which means smallness of the losses of the excited atoms during quenching. Let us calculate this integral for the above-described degree of ionization considering the equality $k_p(t_1)n_e^2(t_1) = [(2T_1/E_1)t_0]^{-1}$:

$$I(\infty) = k_r^e n_0 \alpha_0 \frac{2T_0}{E_l} t_0 \left\{ 1 - \exp\left[-\frac{-E_l}{2T_0 t_0}(t_1-t_0)\right]\right\} +$$
$$+ k_r^e n_1 \alpha_1 t_0 \frac{\operatorname{arctg}\sqrt{E_n/2T_1-1}}{\sqrt{E_l/2T_1-1}} + 2t_0 k_r^a n_c.$$

Here we have set $\gamma = 5/3$, $\mu = 1.5$ for the equilibrium region and $\mu = 1$ for the kinetic region (which has a weak influence on the result, but considerably simplifies the formula). The analysis of this expression indicates that for satisfaction of the condition $I < 1$ it is sufficient to require

$$k_T^e n_0 \alpha_0 t_0 (2T_0/E_1)^{1/2} < 1, \quad 2t_0 k_T^a n_0 < 1.$$

If the opposite inequalities occur, then an exponential decrease in the yield of excited atoms $\varepsilon(\infty)$ occurs as a result of fast relaxation. Consequently, the optimal initial parameters of the plasma must satisfy the expression

$$n_e(0) = (E_1/2T_0)^{1/2}/(k_T^e t_0) = [n_0 K_c(T_0)]^{1/2}, \quad n_0 = 1/(2t_0 k_T^a). \tag{13}$$

It must be noted that for $n_e(0) > n_e^{opt}$ the excited atom concentration after cooling will be no less than for $n_e(0) = n_e^{opt}$ so that the optimalness of the initial parameters is connected with the efficiency of the conversion of the recombination energy into the energy of the excited atoms. The concentration of the excited atoms corresponding to conditions (13) at a temperature T ($T \ll T_0$) will be found by the formula

$$[A^*] = n_e(0)(T/T_0)^{1.5}.$$

Here we have considered that $\varepsilon(\infty)_{T_0^{opt}, n_0^{opt}} = \alpha_0$.

The relations obtained make it possible to estimate the optimal initial parameters of the plasma and the excited atom concentration after cooling for any selected type of atom. The approximate nature of the calculation is primarily connected with representation of the inertial separation of the plasma ($u = const$) and also with neglecting the heat release as a result of recombination. The second approximation, however, is better the closer $\varepsilon(\infty)$ is to α_0. It is necessary to note the good agreement of our estimates with the result of the detailed numerical calculation of [17] performed for the recombining of xenon plasma considering the equations of gas dynamics and the heat release as a result of recombination.

5. For analysis of the possibility of obtaining generation in specific systems it is necessary to have information about the ratio k^*/k, the Einstein

20

coefficient of the electron transition, the spectral constants of the upper and lower states. At the present time the most widely studied are the reactions of the excited atoms of inert gases with halogen-containing molecules. Among the noble gases xenon has the greatest ionization potential. This favors the application of the thermal method of initiation. It is also known that the effectiveness of the formation of electron-excited molecules in the Xe^*+F_2 reaction is close to one, that is, $k^*/k \approx 1$. Therefore let us consider this system as an example of the above-developed concepts.

The lower electron state $XeF(X^1\Sigma^+)$ of the laser transition with $\lambda \sim 350$ nm is characterized by the following parameters: $\omega'' = 250$ cm^{-1}, $D = 1,500$ cm^{-1} [13]. The bound-bound transition takes place to the upper oscillatory levels of this state. The probability of the VT relaxation for one collision calculated by formulas of [14] for $T = 500°$ K (considering the nonadiabatic nature of the collisions) turns out to be on the order of one. Therefore for the estimates we shall assume the existence of dissociated and oscillatory equilibrium of the XeF molecules in the state $X^1\Sigma^+$. Then the condition (9) for $\tau_p = 10^{-7}$ sec, $u = 5 \cdot 10^5$ cm/sec, $h = 1$ cm, $E_v'' = D$ assumes the form

$$(1 - e^{-\omega''/T})[Xe] < 5 \cdot 10^{21}.$$

It turns out that for the XeF molecule in which the transition takes place to the upper oscillatory levels ($E_v'' = D$), condition (9) is satisfied in a wide range of temperatures and concentrations. The role of the temperature is very interesting here. An increase in it leads, on the one hand, to an increase in the degree of population of the vibrational levels, and on the other hand, to a decrease in the molecule concentration in the ground electron state as a result of dissociation. Therefore the condition (9) depends weakly on the temperature at $T > \omega''$. In this case the temperature is limited by the dissociation process of the upper electron state. It is considered that the temperature of the mixture must not exceed 1,000° K [16].

Now let us estimate the possible amplification for the plasma method of creating Xe^*. The initial data for calculating n, T, $[Xe^*]$ are as follows: $k_T^e = 3 \times 10^{-10}$ cm^3/sec [17]; $k_T^a = 10^{-13}$ cm^3/sec; $E_i = 12$ ev; $H = 2$ mm; $u = 5 \cdot 10^5$ cm/sec. Then from (13) we obtain $n_0 = 5 \cdot 10^{18}$ cm^{-3}, $T_0 = 8,000°$ K, $n_e(0) = 3 \cdot 10^{16}$ cm^{-3}. For tenfold cooling (the gas temperature before mixing is 800° K) we shall have $[Xe^*] \approx 10^{15}$ cm^{-3}. In order to calculate the cross section of the induced transition we used the ordinary expression of [12] for the Doppler-broadened line: $\sigma = 10^{-6}(B'M)^{1/2}f(v')/(\tau_{rad}v^3T)$. Here B' is the rotational constant of the upper electron state (cm^{-1}); M is the mass of the molecule (atomic mass units); $f(v')$ is the distribution function with respect to oscillatory levels of the upper electron state; v is the wave number (cm^{-1}). For the radiation lifetime it was established [3, 13] that $\tau_{rad} \leq 10^{-7}$ sec. Therefore for the investigated pressures $\tau_p = \tau_{rad}$ (the decay of the upper state takes place by radiation). In this case the gain does not depend on the quenching rate or on the Einstein coefficient, which is an important characteristic of the resolved transitions. Then for $T = 1,000°$ K we obtain $\sigma\tau_p = 1.2 \cdot 10^{-22}$ cm^2/sec. From formula (8) it follows

21

that the gain $\chi = 6q \cdot 10^{-3}$; for the number of layers $q = 10$, $\chi = 6$ percent. This result makes it possible to hope to obtain generation in the investigated system. A similar analysis demonstrated that in the case of the KrF and ArF molecules the magnitude of the gain will be less.

6. In conclusion, let us discuss the prospects for the creation of chemical lasers based on the reactions of the excited atoms (in addition to the noble atoms). First of all it is necessary to note that the proposed method of formation of the excited atoms can significantly expand the class of reactions by comparison with the pulsed initiation by the electron beam. The latter is limited to the necessity of the preliminary preparation of the reaction mixture which excludes the use of the nonvolatile materials.

As was demonstrated above, the use of atoms with small ionization potentials will permit most complete realization of the possibilities of the thermal method of initiation. This is connected with a decrease in the initial temperature of the gas and, consequently, the degree of cooling which means an increase in density of the excited atoms (see the table). Therefore the atoms of the alkali metals Cs, Rb and Na are of the greatest interest. Unfortunately, only the trimolecular recombination reactions were studied with the participation of these atoms, for example, [6]

$$Cs^* + Xe + Xe \rightarrow CsXe^* + Xe.$$

In order to ensure a sufficient reaction rate, pressures of $\sim 10^3$ mm Hg are required which essentially complicates the mixing of the fluxes. Therefore it appears urgent to find and study bimolecular reactions with the participation of the excited atoms of the alkali metals. The information about the magnitude of the quantum yield of the excited molecules is of the greatest interest.

Another class of reaction systems is made up of the reactions of the group II atoms Zn, Cd and Hg in the metastable states ^3P_J. The most investigated are the photosensitized reactions with the participation of excited mercury atoms [8]. Let us note one type of reaction--the formation of mercury halide molecules--for example, [5]

$$Hg(6^3P_2) + Cl_2 \rightarrow HgCl^*(B^2\Sigma) + Cl.$$
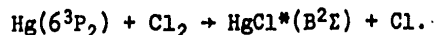
The rate constant of this reaction is close 10^{-10} cm^3/sec. The resolved operating transition $B \rightarrow X$ ($\lambda \sim 500$ nm) ends on the upper oscillatory levels of the ground state ($v'' \sim 20$), which promotes the creation of an inversion. Thus, this reaction corresponds to the general scheme investigated in the given paper. The absence of data on the magnitude of the quantum yield in this reaction does not offer the possibility of calculating the amplification coefficient, but if we consider that $k^*/k \sim 1$, then the gain turns out to be an order larger by comparison with XeF as a result of a decrease in the ionization potential and an increase in the wavelength. The isovalent HgBr, CdCl, ZnCl and other molecules also have an analogous level structure.

The reactions of the formation of these molecules from excited atoms undoubtedly require careful study.

The latest publications investigating chemiluminescence in the $Mg+N_2O$ reactions [19] indicate the defining role of the excited metastable $Mg(^3P)$ atoms in the formation of the electron-excited MgO^* molecules. Accordingly, the above-discussed method of formation of the excited atoms is also of great interest.

In conclusion, it is again necessary to emphasize the possibility of using excited easily ionized Cs, Rb atoms from the point of view of finding the path to the creation of the purely chemical visible laser. The required ionization temperatures of $\sim3,000°$ K actually are obtained on combustion of various fuels, for example, $H_2 + F_2$ [15]. The presented examples indicate the existence of an entire class of systems suitable for the creation of continuous chemical lasers with thermal initiation based on reactions with the participation of electron-excited atoms. The presence of common features both in these reactions and in the lasing molecules permits us to apply the approach developed in this paper to them.

BIBLIOGRAPHY

1. LASER FOCUS, No 12, 1976, p 14.

2. IEEE J., QE-10, 1975, p 690; A. S. Bashkin, N. L. Kupriyanov and A. N. Orayevskiy, KVANTOVAYA ELEKTRONIKA, No 4, 1977, p 1063.

3. J. E. Velazco, J. H. Kolts and D. W. Setser, J. CHEM. PHYS., No 65, 1976, p 3468.

4. M. W. McGeogh, G. R. Furnier and P. Ewart, J. PHYS. B, No 9, 1976, p L121.

5. H. F. Krause and S. G. Jonson, CHEM. PHYS. LETTS, No 31, 1975, p 577.

6. B. Sayer and M. Ferray, J. PHYS. B, No 9, 1976, p L293.

7. L. I. Gudzenko, L. A. Shelepin and S. I. Yakovlenko, TRUDY FIAN, No 83, 1975, p 100.

8. "Vozbuzhdennye chastitsy v khimicheskoy kinetike" [Excited Particles in Chemical Kinetics], Moscow, Mir, 1974.

9. W. Felder, J. CHEM. PHYS., No 56, 1972, p 6028.

10. A. A. Stepanov and V. A. Shcheglov, ZhTF, No 46, 1976, p 563.

11. G. N. Abramovich, "Prikladnaya gazovaya dinamika" [Applied Gas Dynamics], Moscow, Nauka, 1976.

FOR OFFICIAL USE ONLY

12. D. Sutton and S. Suchard, APPL. OPTICS, No 14, 1975, p 1898.

13. B. Ault and L. Andrews, J. CHEM. PHYS., No 65, 1976, p 4192.

14. Ye. Ye. Nikitin, "Teoriya atomno-molekulyarnykh protsessov v gazakh" [Theory of Atomic-Molecular Processes in Gases], Moscow, Khimiya, 1970.

15. A. S. Bashkin, V. I. Igoshin, A. I. Nikitin and A. N. Orayevskiy, "Khimicheskiye lazery" [Chemical Lasers], Moscow, VINITI, 1975.

16. "High-Power Lasers," J. Wiley and Sons, N. Y., 1975.

17. Ye. L. Stupitskiy, ZhTF, No 43, 1973, p 767.

18. Ya. B. Zel'dovich and Yu. P. Rayzer, "Fizika udarnykh voln i vysoko-temperaturnykh gidrodinamicheskikh yavleniy" [Physics of Shock Waves and High-Temperature Hydrodynamic Phenomena], Moscow, Nauka, 1966.

19. D. J. Benard and W. D. Slafer, J. CHEM. PHYS., No 66, 1977, p 1017.

10845
CSO: 8144/0821

FOR OFFICIAL USE ONLY

FOR OFFICIAL USE ONLY

CHAIN-REACTION VISIBLE CHEMICAL LASERS

[Text] A discussion is presented of the problem of creating a chain-reaction visible chemical laser. Radicals (active reaction centers) are proposed as the lasing species. Depopulation of the lower laser level occurs as a result of the chemical reaction. Analysis of the kinetics of the H_2 + NF_2 chain reaction indicates that generation based on the electron transitions of the NF molecule is possible.

1. In the existing infrared chemical lasers, the excited molecules formed in the elementary act of the reaction are at the same time the final product of the reaction. For generation on the vibrational transitions of these molecules their accumulation leads to disruption of the inversion which lowers the efficiency of the use of the chemical energy. This deficiency is manifested especially sharply in the case of chain reactions.

Therefore it appears to be very enticing to use chain reactions in which the molecule formed in the excited stage is the intermediate product (active center). The stationary inversion of such molecules can be realized if the reactivity of the lower laser state is higher than the upper. This situation is more probable for the electron-excited radicals, for the oscillatory excitation, as a rule, leads to an increase in chemical activity. Thus, realization of the proposed system is connected with the creation of visible electron transition chemical lasers. Whereas the reaction of the excited radical limits the rate of the complex process, the presence of the laser field can lead to an increase in the rate of the chain reaction. The process of stimulated emission is organically included in the reaction mechanism.

25

The theoretical conditions of the reazliation of such a system can be formulated as follows: 1) the presence of a chain reaction, in one of the elementary acts of which an electron-excited molecule is formed; 2) this molecule is the intermediate product (active center) in the chain reaction; 3) the reactivity of the molecule in the lower state is greater than in the upper state.

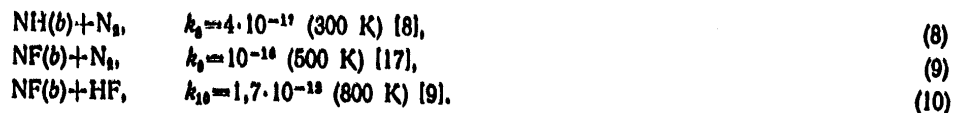The analysis of the experimental and theoretical data performed by us [1-9] demonstrated that the NF and the NH molecules satisfy the last two requirements to a significant degree. These radicals are chemically active and are the intermediate product in many complex processes. The high reactivity of the NF and the NH radicals in the ground triplet state is caused by the presence of two unpaired electrons [1, 3]. The NF and the NH reactions are characterized by the following rate constants (given in cm^3/sec; for brevity the reaction products are not indicated):

$NF(X)+NF(X)$,	$k_1=5\cdot10^{-11}(2300-3000$ K) [2],	(1)
$NF(X)+NF_2$,	$k_2=5\cdot10^{-11}$ (450 K) [3, 4],	(2)
$H+NF(X)$,	$k_3=10^{-11}$ (300 K) [3],	(3)
$NH(X)+NH(X)$,	$k_4=2\cdot10^{-10}$ (1900-2400 K) [2],	(4)
$NH(X)+O_2$,	$k_5=10^{-12}$ (300 K) [2, 6],	(5)
$NH(X)+NH_3$,	$k_6=2\cdot10^{-11}$ (300 K) [5].	(6)
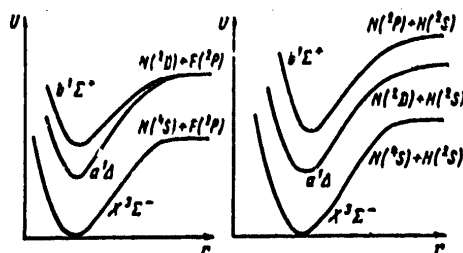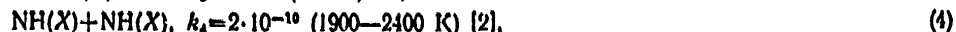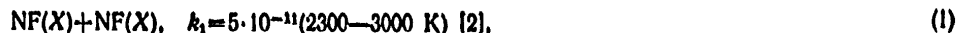
On the other hand, in the excited states of $NF(a^1\Delta, 1.4$ ev; $b^1\Sigma, 2.3$ ev) and $NH(a^1\Delta, 1.6$ ev; $b^1\Sigma, 2.7$ ev) (see the figure) the electrons are paired, which leads to a significant retardation of the corresponding reactions:

$NF(a)+NF(a)$,	$k_{1a}=10^{-12}$ (800 K) [3, 7],	(1a)
$NF(a)+NF_2$,	$k_{2a}=2\cdot10^{-13}$ (450 K) [3, 4],	(2a)
$NF(b)+NF_2$,	$k_{2b}=5\cdot10^{-13}$ (450 K) [3, 4],	(2b)
$NF(a)+H$,	$k_{3a}=10^{-12}$ (300 K) [3],	(3a)
$NH(b)+O_2$,	$k_{5b}=2,4\cdot10^{-14}$ (300 K) [8],	(5b)
$NH(b)+NH_3$,	$k_{6b}=4\cdot10^{-13}$ (300 K) [8],	(6b)
$NH(b)+Ar$,	$k_7=5\cdot10^{-14}$ (300 K) [8],	(7)

$NH(b)+N_2$,	$k_8=4\cdot10^{-17}$ (300 K) [8],	(8)
$NF(b)+N_2$,	$k_9=10^{-14}$ (500 K) [17],	(9)
$NF(b)+HF$,	$k_{10}=1{,}7\cdot10^{-13}$ (800 K) [9].	(10)

In addition, the states a and b have high resistance to extinguishing colli-
sion (processes (7)-(10)). In this sense they are analogous to the known
singlet states $O_2:a^1\Delta g$, $b^2\Sigma g$.

2. Now let us discover the condition of existence of the stationary inver-
sion on the electron transition during the course of the chemical reaction.
In the investigated molecules, the transitions a-X and b-X of interest to us
take place in accordance with the Frank-Condon rule between the most popu-
lated basic vibrational levels. The only possible mechanism of supporting
the stationary inversion consists in predominant depopulation of the basic
electron state of the molecules. The ratio of the reaction rates for the
ground and excited states determines the quantum yield of the electron-
excited molecules in the pumping reaction required for formation of the in-
version. Departing from the vibrational-rotational structure of the transi-
tion (which has no effect on the result), it is possible to obtain the fol-
lowing condition of the stationary inversion:

$$\frac{R^*}{R_0} > g^* \frac{\sum_i k_i^*[M_i] + \sum_i k_{ii}[M_i] + w_{rad}}{\sum_i k_i^0[M_i]},$$

where R^*, R_0 are the reaction rates with the formation of excited and unex-
cited molecules; g^*, g_0 are the statistical weights of the electron states;
k_i^*, k_i^0 are the rate constants of the chemical reactions of the excited and
unexcited molecules with a component of the mixture M_i; k_{ti} is the rate con-
stant of extinguishing the excited state to the ground state; w_{rad} is the
probability of spontaneous radiation transition. For NF and NH molecules,
the decay of the metastable states a and b ($w_{rad} \leq 10^2$ sec^{-1}) is determined
only by the reactions. The threshold efficiency of the formation of the ex-
cited particles R^*/R_0 depends, generally speaking, on the composition of the
reacting mixture. If a predominant process exists (for example, the reac-
tions (2), (2a), (2b) for NF or (6), (6b) for NH), then for a quantum yield
of $\eta = R^*/(R^* + R_0)$, for which inversion occurs, it is possible to obtain
the following conditions: for NF $\eta(a^1\Delta) > 0.03$, $\eta(b^1\Sigma) > 0.03$; for NH
$\eta(b^1\Sigma) > 0.01$. As is known [9], the quantum yield of the electron excita-
tion in many exothermal reactions reaches a magnitude of tens of percentages,
which also indicates the reality of the mechanism of formation of the inver-
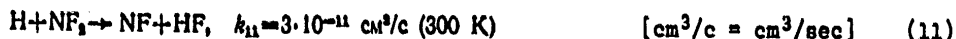sion investigated here.

The similarity of the reaction properties of the isoelectronic NH and NF
radicals permits proposal of the presence of analogous properties also for
the PH, PF, AsH and AsF radicals having similar structure of the lower elec-
tron states (the corresponding transitions also occur in the visible band).

27

These molecules have larger induced radiation cross sections than NH and NF as a result of partial removal of the ban on intercombination transitions in heavier molecules. It is known that the enumerated radicals are short-lived intermediate products in many exothermal chain processes [1]. Thus, for example, the transition $PH(b^1\Sigma \rightarrow X^3\Sigma^-)$ was observed in flames of white phosphorus with hydrogen [10], and in the reactions $PH_3(AsH_3)$ with F_2, glow of the PF and AsF radicals was observed [11].

3. Now let us proceed to the investigation of the chain reaction in which electron-excited molecules are formed. The best-studied reactions are those with the participation of NF; therefore this radical will be used as an example in further discussion.

It is known [3] that the yield of excited $NF(a^1\Delta)$ molecules in the reaction

$$H + NF_2 \rightarrow NF + HF, \quad k_{11} = 3 \cdot 10^{-11} \text{ cm}^3/\text{c} \text{ (300 K)} \qquad [\text{cm}^3/\text{c} = \text{cm}^3/\text{sec}] \qquad (11)$$

is close to 100 percent. Such high efficiency of obtaining the electron excitation is connected with the specific mechanism of the reaction occurring through the singlet excited state of the HNF^* molecule (^1A) with subsequent decay of it into $NF(^1\Delta)$ and $HF(^1\Sigma)$. The formation of $NF(X^3\Sigma)$ is forbidden by the rule of conservation of spin. On the other hand, the inhibition of explosion by negligible additions of hydrocarbons and the presence of two combustion limits observed experimentally [12, 13] indicate the chain mechanism of the complex reaction $H_2 + N_2F_4$. It is not N_2F_4 that participates in the elementary acts, but the NF_2 radical. The latter fact is connected with the low energy of the NF_2-NF_2 bond ($\sim$20 kcal/mol), which leads to significant dissociation of it already at low temperatures (for T = 500° K and p = 20 mm Hg the degree of dissociation is close to 100 percent).
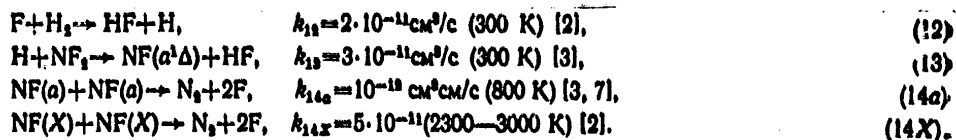
An analysis of the experimental data of [12-14] makes it possible to isolate two stages in the complex reaction $H_2 + N_2F_4 + NF_2$. We shall consider the case of external initiation of the reaction under the conditions of suppression of the branching of the chain by the inhibitor additives. In the first stage where the temperature of the mixture does not exceed 1,000° K, a simple chain reaction takes place with radical links with the participation of NF(a, X), F, H, NH (the corresponding elementary acts have an activation energy of $\leq$2 kcal/mol), which is accompanied by heating of the mixture and dissociation of $N_2F_4 \rightarrow 2NF_2$. Inasmuch as the NF_2 radical is much more active than the N_2F_4 radical, the dissociation leads to acceleration of the reaction.

The elementary reaction with high energy of activation "are included" in the second stage (for T $\geq$ 1,000° K): $H_2 + NF_2$ (36 kcal/mol), $NF_2 \rightarrow NF + F$ (60 kcal/mol), and so on. A thermal explosion actually takes place. This regime is harmful for the laser, for at high temperature the rate constant k_1^* and k_1^0 compare, and the reaction (11) ceases to dominate in the formation of the NF. Both of these factors can lead to interruption of inversion. Therefore, considering the mixture a sufficiently dilute inert gas for superheating
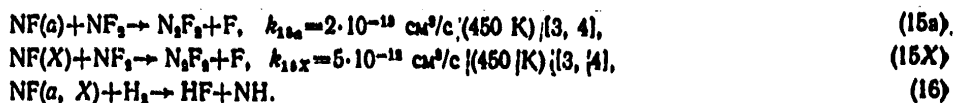
28

conversion, let us limit ourselves to the investigation of the radical stage of the complex reaction $H_2 + NF_2$.
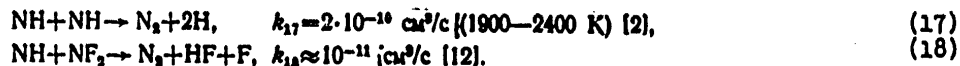
The elementary acts of formation of the chain do not play a role for the reaction initiated by the side source. Out of a large number of possible elementary acts in the complex reaction [12-14] we selected only the fastest process of continuation of the chain, defining the kinetics of the system in the investigated regime:

$F + H_2 \rightarrow HF + H$, $\quad k_{12} = 2 \cdot 10^{-11} \text{cm}^3/\text{c}$ (300 K) [2], $\qquad$ (12)

$H + NF_2 \rightarrow NF(a^1\Delta) + HF$, $\quad k_{13} = 3 \cdot 10^{-11} \text{cm}^3/\text{c}$ (300 K) [3], $\qquad$ (13)

$NF(a) + NF(a) \rightarrow N_2 + 2F$, $\quad k_{14a} = 10^{-12} \text{cm}^3 \text{cm}/\text{c}$ (800 K) [3, 7], $\qquad$ (14a)

$NF(X) + NF(X) \rightarrow N_2 + 2F$, $\quad k_{14x} = 5 \cdot 10^{-11}$(2300—3000 K) [2]. $\qquad$ (14X).

The value of k_{14x} is constant in the temperature range of 2,300-3,000° K, which indicates the low energy of activation and, consequently, high reaction rate for $T \leq 1,000°$ K.

$NF(a) + NF_3 \rightarrow N_2F_2 + F$, $\quad k_{15a} = 2 \cdot 10^{-12} \text{cm}^3/\text{c}$ (450 K) [3, 4], $\qquad$ (15a),

$NF(X) + NF_3 \rightarrow N_2F_2 + F$, $\quad k_{15x} = 5 \cdot 10^{-12} \text{cm}^3/\text{c}$ (450 K) [3, 4], $\qquad$ (15X)

$NF(a, X) + H_2 \rightarrow HF + NH$. $\qquad$ (16)

The data from [9] permit the following estimate to be made: $k_{16x} < 6 \cdot 10^{-14}$ cm^3/sec (800° K). However, the appearance of the NH radical in the mixture $N_2F_4 + NF_2 + H_2$ was observed in [12] immediately after the photolytic pulse (delay time less than 10 microseconds for $[H_2] = 4 \cdot 10^{17}$ cm^{-3}, T ≈ 500° K). Hence, it is possible to obtain a value of $k_{16x} > 2 \cdot 10^{-13}$ cm^3/sec (500° K). It is important that in the reaction (16), the NH radical is formed in the active triplet state inasmuch as the energy of the reaction is insufficient for effective excitation of $NH(^1\Delta)$. This leads to fast continuation of the chain through NH in the mixtures rich in hydrogen:

$NH + NH \rightarrow N_2 + 2H$, $\quad k_{17} = 2 \cdot 10^{-10} \text{cm}^3/\text{c}$ (1900—2400 K) [2], $\qquad$ (17)

$NH + NF_2 \rightarrow N_2 + HF + F$, $\quad k_{18} \approx 10^{-11} \text{cm}^3/\text{c}$ [12]. $\qquad$ (18)

Under the conditions of a reaction initiated by an external source (in the presence of high concentrations of the radicals) the basic process of breaking the chain is the bimolecular reaction

$NF(a, X) + H \rightarrow HF + N$, $k_{19a} = 10^{-12} \text{cm}^3/\text{c}$, $k_{19x} = 10^{-11} \text{cm}^3/\text{c}$ [3]. $\qquad$ (19)
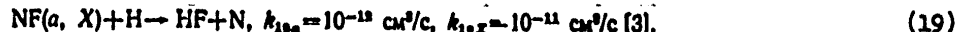
The effect of reaction (19) on the total concentration of the active centers can be neglected if the chain-breaking rate $k_{19x}[NF(X)][H] + k_{19a}[NF(a)][H]$ is much less than the rate of continuation of the chain $k_{13}[H][NF_2]$ and $k_{15x}[NF(X)][NF_2]$. These conditions are satisfied if the degree of initiation (the ratio of the total concentration of the radical to $[NF_2]$) does not exceed ~10 percent.

FOR OFFICIAL USE ONLY

The processes of extinguishing the NF molecule from the state $a^1\Delta$ to the state $X^3\Sigma$ also must be considered in the kinetics of the chain reaction. The basic decay channel NF(a) on collision with the molecules of the initial reagents H_2, NF_2 is the reactions (15a) and (16a). The collisions with the HF and the N_2 molecules, on the contrary, lead only to extinguishing:

$$NF(a) + HF \rightarrow NF(X) + HF, \quad k_{20} < 10^{-13} \text{ cm/c (800 K) [9]},$$ (20)

$$NF(a) + N_2 \rightarrow NF(X) + N_2, \quad k_{21} < 10^{-16} \text{ cm}^3\text{/c (500 K) [4]}.$$ (21)

The analysis of the elementary acts (12)-(21) indicates that in the $H_2 + NF_2$ mixture a chain reaction takes place on initiation by an external source. In one of the acts of continuation of the chain, the electron-excited molecules NF(a) are formed. The advantages of chain reactions in chemical lasers are exhibited only when the time of existence of the stationary inversion is comparable to the time of the chain chemical process. In other words, the laser length of the chain must be close to chemical. Therefore in order to estimate the prospectiveness of the given system it is necessary to discover the behavior and possible causes of the discontinuation of inversion during the course of the chain reaction. For this purpose let us write the balance equations for the concentrations of the active centers considering the induced transitions under the effect of a light field of intensity I (photons/cm^2-sec). For simplicity let us neglect the generation of H_2 and NF_2, the rate of variation of the temperature and concentration of the products and also the contribution of the reactions (16)-(18). The last approximation is completely justified in the absence of a field in view of the smallness of the constant k_{16a}. In the saturation mode, consideration of the reactions (16)-(18) does not lead to theoretical variations as will be clear from the further discussion. In addition, in the initial stage of the reaction it is possible to neglect the breaking of the chain. The corresponding equations are written as follows:

$$d[F]/dt = k_{15a}[NF(a)][NF_2] + k_{15x}[NF(X)][NF_2] + 2k_{14a}[NF(a)]^2 +$$
$$+ 2k_{14x}[NF(X)]^2 - k_{11}[F][H_2], \quad d[H]/dt = -k_{11}[H][NF_2] + k_{13}[F][H_2],$$
$$d[NF(a)]/dt = -\sigma I \{[NF(a)] - \tfrac{3}{2}[NF(X)]\} + k_{13}[H][NF_2] -$$
$$- [NF(a)] \sum_i k_{ii}[M_i] - k_{15a}[NF(a)][NF_2] - 2k_{14a}[NF(a)]^2,$$

$$d[NF(X)]/dt = \sigma I \{[NF(a)] - \tfrac{3}{2}[NF(X)]\} + [NF(a)] \sum_i k_{ii}[M_i] -$$
$$- k_{15x}[NF_2][NF(X)] + 2k_{14x}[NF(X)]^2,$$
$$[F] + [H] + [NF(a)] + [NF(X)] = A,$$

where σ is the cross section of the induced radiation for the transition a-X; A is the concentration of the active centers created by the external source at the initial point in time. In the quasistationary approximation [1] all of the derivatives are equal to zero, as a result of which a system of algebraic equations is obtained. Its solution (quite awkward) can be described in explicit form, but the physical meaning of the formulas is clearer

if we omit the quadratic terms with respect to [NF(a)] and [NF(X)]. The estimates indicate the admissibility of this approximation for $A/[NF_2] < 10^{-1}$. Let us consider the most interesting consequences from the solution. Thus, for example, the formula for the density of the inversion $\Delta = [NF(a)] - (2/3)[NF(X)]$ assumes the form

$$\Delta = \frac{A\left(k_{16}x[NF_a] - {}^2/_a \sum_i k_{ii}[M_i]\right)}{(\gamma_X + {}^2/_a\gamma_a)\sigma I + k_{16}x[NF_a]\gamma_a + \gamma_X \sum k_{ii}[M_i]} , \tag{22}$$

where $\gamma_{a(X)} = \left(\frac{[NF_a]k_{16a}(X)}{[H_a]k_{1a}} + \frac{k_{16a}(X)}{k_{1a}} + 1\right)$ take into account the contribution of the [F] and [H] to the total concentration of the active centers so that $\gamma_X[NF(X)] + \gamma_a[NF(a)] = A$ (for $[NF_2] \approx [H_2]$, $\gamma_a \approx 1$, $\gamma_X \approx 2$).

From (22) for

$$I \ll \frac{k_{16}x[NF_a]\gamma_a + \gamma_X \sum_i k_{ii}[M_i]}{\sigma(\gamma_X + {}^2/_a\gamma_a)} \approx I_s$$

(I_s is the saturating intensity) we have the formula for the unsaturated inversion density under steady-state conditions:

$$\Delta_0 = \frac{A\left(k_{16}x[NF_a] - {}^2/_a \sum_i k_{ii}[M_i]\right)}{k_{16}x[NF_a] + \gamma_X \sum_i k_{ii}[M_i]} .$$

This expression makes it possible to draw some important conclusions.

First, the interruption of inversion takes place when the depopulation rate of the lower laser level $k_{15}x[NF_2]$ becomes less than the total extinguishing rate $\sum_i k_{ti}[M_i]$. Inasmuch as all of the k_{ti} are much smaller than $k_{15}x$, this is possible only for $[NF_2] \ll [M_i]$, that is, for in practice complete burnup of the reagents. During the course of the reaction, the approximate equality $\Delta_0 \approx A$ is satisfied which means that [NF(a)] essentially exceeds the concentration of the remaining radicals. The cause is smallness of the reaction rates with the participation of NF(a) and the extinguishing processes by comparison with the other processes. The extinguishing and chemical depopulation of the state $a^1\Delta$ are compensated for by the pumping reaction.

Secondly, the absolute magnitude of the inversion can decrease in the reaction process as a result of breaking of the reaction chain in (19). However, this effect can play a role only for a significant degree of burnup of the reagents (see above).

Taken together, the enumerated conclusions mean the following: if sufficient density of the radicals for satisfaction of the condition of self-excitation

can be created in the H_2 + NF_2 system, the generation time will be on the order of the time of occurrence of the chemical chain reaction which theoretically can ensure high chemical efficiency of the system.

4. It is interesting to trace how the rate of a complex reaction $R = |d[H_2]/dt|$ varies as a function of the light field intensity:

$$R = \frac{A\,[NF_2]\left\{\sigma I\,(^1/_2 k_{15a} + k_{15}x) + k_{15}x \sum_i k_{ii}[M_i] + k_{15}x k_{16a}[NF_2]\right\}}{(\gamma_x + {}^2/_3\gamma_a)\sigma I + k_{15}x[NF_2]\,\gamma_a + \gamma_x \sum_i k_{ii}[M_i]}.$$

For I = 0, R = $A[NF_2]k_{15a}$, that is, the reaction rate is limited to the slow element (15). In the saturation mode for I >> I_s we have R = $A[NF_2]k_{15x}/2$. Inasmuch as k_{15x}/k_{15a} = 20, the reaction rate increases by approximately 10 times.

The formulas obtained make it possible to find the quantum yield of the stimulated emission α in the chemical reaction (α = P/R, where P is the power of the stimulated emission c of unit volume, and R is the reaction rate coinciding with the pumping power of the state $a^1\Delta$). Under quasistationary conditions the value of P is determined by the expression

$$P = \sigma I\,\{[NF\,(a)] - {}^2/_3[NF\,(X)]\} = k_{15}x[NF_2][NF\,(X)] + 2k_{16}x[NF\,(X)]^2 -$$
$$- [NF\,(a)]\sum_i k_{ii}[M_i].$$

In the saturated generation or amplification mode the inversion density is maintained on the level of the threshold Δ_π. For amplification Δ_π = 0, and in the generator Δ_π = $(\sigma c \tau_\phi)^{-1}$ (τ_ϕ is the lifetime of a photon in a resonator). The threshold condition $[NF(a)]$ - (2/3)[NF(X)] = Δ_π together with the equality $\gamma_x[NF(X)]$ + $\gamma_a[NF(a)]$ = A permits us to find [NF(X)] and [NF(a)], and then P and R. The final result for α has the form

$$\alpha = \frac{k_{15}x[NF_2]\,(A - \gamma_a\Delta_a) - (\Delta_\pi\gamma_x + {}^2/_3A)\sum_i k_{ii}[M_i]}{k_{15}x[NF_2]\,(A - \gamma_a\Delta_n) + k_{16a}[NF_2]\,(\Delta_\pi\gamma_x + {}^2/_3A)}. \tag{23}$$

From (23) we have the following important corollary: for effective energy output it is necessary either to ensure sufficiently powerful initiation in the laser (A >> $\gamma_a\Delta_\pi$) or to operate in the amplifier mode where Δ_π = 0.

Before proceeding to the specific initiation systems of the laser, it is necessary to determine the amplification index as a function of the concentration of the electron-excited NF molecules in order then to find the threshold density of the inversion. As is demonstrated in [15], the amplification index for the electron transition of a diatomic molecule (Λ', S', v') → (Λ'', S", v") optimize with respect to the rotational quantum numbers can be represented as follows in the case of Doppler broadening:

FOR OFFICIAL USE ONLY

$$\varkappa\,[\text{CM}^{-1}] = \frac{2,7\cdot10^{-6}[B'\,M]^{1/2}q_{v',\,v'}}{\tau_{\text{rad}}v^3T}\left[f'(v')N' - \frac{(2-\delta_{\Lambda',\,2})}{(2-\delta_{\Lambda'',\,2})}\frac{(2S'+1)}{(2S''+1)}f''(v'')N''\right],$$

where Λ, S are the quantum numbers of the electron states; v is the number of the vibrational level; B' is the rotational constant of the upper state, cm^{-1}; M is the mass of a molecule, amu; v is the wave number, cm^{-1}; T is the progressive temperature, K; τ_{rad} is the radiation lifetime, sec; $g_{v'}$, v'' is the Frank-Condon factor; f', f'' are the distribution functions with respect to vibrational level; N', N'' are the populations of the upper and lower electron states. For NF(a), NF(b) it has been established experimentally that when $T < 1,000°$ K, $f'(0) \gg f'(v' \neq 0)$ and, in addition, $q_{0,\,0} \gg q_{0,\,v''\neq0}$ [17]. Therefore, considering only the transition $v' = 0 \rightarrow v'' = 0$, for $N' > N''$ we obtain

$$\varkappa(a \rightarrow X) = 2,6\cdot10^{-20}[\text{NF}(a)], \quad \lambda = 874 \text{ nm};$$
$$\varkappa(b \rightarrow X) = 3,7\cdot10^{-19}[\text{NF}(b)], \quad \lambda = 528 \text{ nm}$$

for the following values of the parameters: $T = 500°$ K, τ_{rad} ~ 15 milliseconds ($b^1\Sigma$) and 1 sec ($a^1\Delta$) [7]; $B'(a) = B'(b) = 1.22$ cm^{-1}. Let us note that the amplification index for the transition NH $b \rightarrow X$ is $5 \cdot 10^{-19}$ [NH($b^1\Sigma$)].

5. The base for practical use of the H + NF mixture is its above-noted "metastability."

The reaction of generation of the $H_2 + NF_2 \rightarrow HNF_2 + H$ chain has an activation energy of 36 kcal/mol. Therefore there is a temperature range in which the N_2F_4 molecules are dissociated, and there is no explosion (of course, if the branching processes are compensated for by the addition of an inhibitor). This fact was most clearly exhibited in the experiment described in [13], where a mixture of 40 mm Hg of H_2 + 20 mm Hg of N_2F_4 + 0.014 mm Hg of C_4H_8 did not explode in 10 minutes on being heated to 110° C. Under the conditions of this experiment, the degree of dissociation of the N_2F_4 was 50 percent, and the time of establishment of the equilibrium with respect to dissociation was 5 sec [17].

The mixture prepared in this way can be initiated photolytically. The NF photoabsorption cross section (with dissociation into NF + F) is 10^{-18} cm at a maximum for $\lambda = 260$ nm and $\Delta\lambda$ ~ 20 nm [12]. The flux of 10^{22} photons/cm^2-sec into the absorption band of NF_2 (characteristic for chemical lasers with F_2) permits us to create a concentration of active centers of ~$2 \cdot 10^{17}$ cm^{-3} for $[NF_2] = 10^{18}$ cm^{-3} in the time ~10 microseconds. As was demonstrated above, in this case the concentration of $[NF(a)]$ ~ $2 \cdot 10^{17}$ cm^{-3} must be formed which corresponds to the amplification index of ~10^{-2} cm^{-1}.

Of course, the system proposed here is not the only one, which only emphasizes the attractiveness of using the $H_2 + NF_2$ reaction in chemical lasers. For example, there is an interesting possibility of initiating the $N_2F_4 + H_2$ mixture by the radiation of a CO_2 laser (N_2F_4 and NF_2 absorb 10.6-micron emission well). In [14] this procedure was used to obtain amplification on

33
FOR OFFICIAL USE ONLY

the vibrational transitions of HF. However, in order to create the NF laser
a statement of the experiment different from [14] is required. The thermal
dissociation of $N_2F_4 \rightarrow 2NF_2$ can be realized on irradiation with intensity
less than threshold [20]. Then it is necessary to introduce a powerful
pulse of the CO_2 laser into a mixture of $NF_2 + H_2$ (with an intensity above
threshold) which also realizes initiation of an explosive chain reaction.

The mixing of the fluxes of atomic fluorine with H_2 and NF_2 [7] or fluxes of
H with NF_2 also is a possible means of obtaining inversion. However, in
this case the small amplification cross section and the necessity to have
high concentrations of NF(a) and the radicals give rise to quite rigid re-
quirements on the mixing conditions of the fluxes.

When using the transition b → X in NF($\lambda \approx 520$ nm) as the laser transition,
a threshold concentration of the excited molecules of an order less than in
the case of NF(a) is required. This fact forces us to find methods of ex-
citing NF(b). The chemical excitation of the stage $b^1\Sigma$ was observed in
various reactions [3, 17], but there is no information about the efficiency
of its formation. Obviously, the excitation of the NF(b) takes place from
the state $a^1\Delta$ as a result of energy transfer from certain chemically excited
particles [3, 17]. It is possible to use this pumping procedure to create a
laser based on the b → X transition. The necessity for an additional pump-
ing process of a → b, of course, complicates the system by comparison with
the simple chain reaction for NF(a).

As was reported in [16], the resonance process

$$NF(a^1\Delta) + J^*(^2P_{1/2}) \xrightarrow{k_\pi} NF(b^1\Sigma) + J(^2P_{1/2})$$
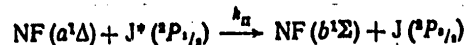
has a gas-kinetic cross section, that is $k_\pi \sim 10^{-10}$–10^{-11} cm^3/sec. Mixing
the excited iodine flux [18] in the reacting mixture of $H_2 + NF_2$ is one of
the methods of creating excited NF(b) molecules.

Another interesting possibility is connected with the characteristic conver-
sion of the emission of an iodine laser on a wavelength of $\lambda = 1.3$ microns.
The presence of a small addition of atomic iodine in the reacting mixture of
$H_2 + NF_2$ leads to the appearance of $I^*(^2P_{1/2})$ on irradiation of it by 1.3-
micron emission and, consequently, it leads to pumping of the NF(b) in ac-
cordance with the formula

$$I(^2P_{1/2}) \xrightarrow{1.3\ \mu} I^*(^2P_{1/2}) \xrightarrow{(+NF(a))} NF(b).$$
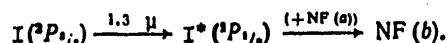
The proposed formula can serve as an effective "adder" of two quanta: 1.3
microns from the iodine laser and 0.87 micron obtained as a result of the
chemical chain reaction.

6. In conclusion, let us note the events of greatest interest in practical
respects. First of all, the class of diatomic radicals attracts attention

FOR OFFICIAL USE ONLY

for which the chemical reaction rates for the basic triplet state are essen-
tially higher than for the excited singlets (NF, NH and other molecules).
Such radicals are intermediate products in many complex exothermal reactions
frequently occurring by the chain mechanism. The relatively low energy of
the singlet excited states $a^1\Delta$, $b^1\Sigma$ gives rise to the possibility of their
excitation in the chemical reactions, and the increased reactivity of the
ground state permits us to hope for the formation of stationary inversion of
the singlet-triplet transition as a result of chemical depopulation of the
lower (ground) state.

The use of the H_2 + NF_2 reaction with the operating NF molecule is the most
realistic way to realize this schematic. The attractiveness of this reac-
tion consists in the possibility of preparing a stable operating mixture and
a variety of initiation techniques (photolysis, mixing of the reagents, ini-
tiation by CO_2 laser emission). It is necessary to note that the mixture of
D_2 + N_2F_4 + NF_2 was already used to obtain pulse generation on the vibra-
tional transitions of the DF molecule, but the laser effect was caused by
the nonchain chemical reaction which it is possible to explain by the small-
ness of the partial concentration of NF_2 under the experimental conditions
[19]. Inasmuch as the reaction of H_2 + NF_2 can be initiated by the atomic
fluorine flux, there is a possibility for creating a purely chemical laser
based on electron transitions. For this purpose it is necessary to use the
methods of obtaining F developed for continuous-action chemical lasers oper-
ating in the infrared range on the basis of the hydrogen fluoride reaction.

One of the interesting peculiarities of the given system is the dependence
of the complex reaction rate on the magnitude of the resonance light field,
which leads to the realization of a characteristic variety of photostimu-
lated reactions. This effect can theoretically be detected with respect to
an increase in intensity of the chemiluminescence of the HF molecule by
$\lambda \sim 3$ microns for occurrence of the reaction in the resonator of any laser,
the operating wavelength of which is in resonance with the a-X transition in
the NF molecule.

BIBLIOGRAPHY

1. V. N. Kondrat'yev and Ye. Ye. Nikitin, "Kinetika i mekhanizm gazofaz-
   nykh reaktsiy" [Kinetics and Mechanism of Gas-Phase Reactions], Moscow,
   Nauka, 1974.

2. V. N. Kondrat'yev, "Konstanty skorosti gazofaznykh reaktsiy" [Rate Con-
   stants of Gas-Phase Reactions], Moscow, Nauka, 1970.

3. J. M. Herbelin, CHEM. PHYS. LETTS, No 42, 1976, p 367.

4. R. J. Collins and D. Nusain, J. PHOTOCHEM., No 2, 1972, p 459.

5. C. Zetzsch and F. Stuhl, J. CHEM. PHYS., No 66, 1977, p 3107.

35
FOR OFFICIAL USE ONLY

6. D. W. Cornell, J. AMER. CHEM. SOC., No 88, 1966, p 544.

7. J. M. Herbelin, D. J. Spencep and M. A. Kwok, J. APPL. PHYS., No 48, 1977, p 3050.

8. B. Gellernt, J. CHEM. PHYS., No 65, 1976, p 4940.

9. "Electronic Tansition Lasers," MIT Press, 1976.

10. E. B. Ludlam, J. CHEM. PHYS., No 3, 1935, p 617.

11. G. L. Schott and S. W. Rabideau, IEEE J., QE-11, 1975, p 690.

12. V. M. Zamanskiy, candidate's dissertation, Moscow State University, 1975.

13. L. Kuhn and C. Wellman, INORG. CHEM., No 9, 1970, p 602.

14. J. L. Lyman and R. J. Jensen, J. PHYS. CHEM., No 77, 1973, p 883.

15. D. G. Sutton and S. N. Suchard, APPL. OPTICS, No 14, 1975, p 1898.

16. M. K. Kwok, LASER FOCUS, No 12, 1976, p 18.

17. M. A. Clyne and I. F. White, CHEM. PHYS. LETTS, No 6, 1970, p 465.

18. P. Cadman and J. Polanyi, J. PHYS. CHEM., No 72, 1968, p 3715.

19. N. G. Basov, V. T. Galochkin, L. V. Kulakov, Ye. P. Markin, A. I. Nikitin and A. N. Orayevskiy, KVANTOVAYA ELEKTRONIKA, edited by N. G. Basov, No 4, 1971, p 50.

20. N. G. Basov, Ye. P. Markin, A. N. Orayevskiy, A. V. Pankratov and A. N. Skachkov, PIS'MA V ZhETF, No 14, 1971, p 251.

10845
CSO: 8144/0821-22

FOR OFFICIAL USE ONLY

FEASIBILITY OF A GAS-DYNAMIC LASER OPERATING ON TRANSITIONS BETWEEN TWIN CO$_2$ MODE LEVELS

[Article by V. K. Konyukov and V. N. Fayzulayev, Physics Institute imeni P. M. Lebedev of the USSR Academy of Sciences, Moscow; submitted 28 December 1977]

[Text] Previous reports [1, 2] have been published on the feasibility of amplifying radiation in the $\lambda \approx 19$ micron range on the vibrational-rotational (03^10)-(100) transitions of the CO$_2$ band. The inverse population on this transition occurs as a result of the Trinor molecule distribution with respect to levels of the CO$_2$ twin modes which include the randomly degenerate longitudinal v_1 and bending v_2 symmetric vibrations. In [2] the corresponding estimates were made of the parameters of the active medium and the electric pumping power for the direct-flow version of a CO$_2$ gas discharge laser in which the low temperature (T = 150° K) operating conditions were ensured by an argon coolant. However, the amplification coefficient on the (03^10)-(100) transition was small as a result of the sharp dilution of the carbon dioxide by the argon (CO$_2$:Ar = 1:50). Accordingly, it is of interest to estimate the feasibility of using thermal pumping of the active medium in the gas-dynamic version of a CO$_2$ laser on the twin mode levels.

As is known, for occurrence of inverse population with the Trinor molecule distribution with respect to levels significant vibrational nonequilibrium is required under low gas temperature conditions. In the investigated case the nonequilibrium must be such that the following expression is satisfied [1]

$$\frac{T_{12}}{T} \gg \left[1 - \frac{E_{n+1,\lambda} - E_{v,\beta}}{\hbar\omega_2} \right]^{-1} , \qquad (1)$$

where T_{12} is the effective twin mode temperature which in the harmonic approximation determines the general quantum reserve l_{12} of the symmetric vibrations v_1, v_2 of the CO$_2$ molecule; $\hbar\omega_2$ is the quantum energy of a bending vibration; $E_{v\beta} = E_{v_1 v_2^1 0}$ is the energy of the β-component of the multiplet with the vibration number $v = 2v_1 + v_2$.

Thus, for example, for the $(03^{1}0)$, (100) levels which belong to the multiplets with $v = 3$ and 2 and which are shifted with respect to their centers by the energy $E_{v_1 v_2^{1}0} = E_{v_1 v_2^{1}0} - (2v_1 + v_2)\hbar\omega_2$ equal respectively to -70 and

50 cm^{-1}, the population inversion according to (1) is possible at $T_{12}/T \gtrsim 5$. In essence, (1) is the analog of the condition of partial inversion on the vibrational-rotational transitions of diatomic molecules. With the gas-dynamic method of thermal pumping of the active medium, the satisfiability of this condition is ensured by the effect of freezing the symmetric vibrations which occurs in the process of adiabatic expansion of the gas through a supersonic nozzle or slit. In order to achieve the required discontinuity of the vibrational temperature T_{12} and the gas temperature, it is expedient to introduce a relatively small amount of argon ([Ar] $\sim$ 50 percent) into the gas mixture, which, without essentially influencing the relaxation process rates, offers the possibility of significantly increasing the rate and depth of cooling of the gas in the supersonic flow.

The results are presented below from a numerical solution of the kinetic equations describing the vibrational relaxation of the mixture of CO_2:Ar = 1:1 expanding through a slit into a vacuum in the approximation of the thermodynamic model of CO_2 [3]. The flow of gas mixture was assumed, just as in [4], to be isentropic with an effective adiabatic index γ corresponding to instantaneous freezing of all of the CO_2 vibrations. The data presented in [5] were used for the rate constants of the relaxation processes. The vibrational inverse population $\Delta N = N_{03^{1}0} - N_{100}$, and the amplification index α at the transition $(03^{1}0)-(100)$ were calculated in the approximation of Trinor molecule distribution with respect to levels $(v_1 v_2^{1}0)$ of the twin modes of CO_2:

$$ N_{v_1 v_2^{1}0} = N_{000}\exp\left[-(2v_1 + v_2)\frac{\hbar\omega_2}{T_{12}} - \frac{\Delta E_{v_1 v_2^{1}0}}{T} \right]g_l, $$

where $g_l = 1$ if $l = 0$; $g_l = 2$ if $l \neq 0$. The rotational distribution temperature was assumed to be equal to the gas temperature. The data on the impact broadening cross sections and the probability of the radiation transition were taken from [2].

The standard relations are presented in Figure 1 for the vibrational inverse population ΔN and the amplification index α for the P(15)-branch of the $(03^{1}0)-(100)$ band as a function of distance to the slit ξ expressed in calibers: $\xi = x/h$, where $h = 0.04$ cm is the half-width of the slit. The behavior of the gas temperature T and the vibrational temperatures of the symmetric vibrations T_{12} and the antisymmetric vibrations T_3 along the axis of the jet is also illustrated in Figure 1. Let us note that the high pumping level of the symmetric vibrations and the low gas temperatures characteristic of the expansion of a CO_2-Ar gas mixture through a slit make it possible to realize inversion in the jet also at other transitions. Thus, in particular for $T_{12}/T_H \gtrsim 12$ the amplification with $\alpha \sim 0.1$ cm^{-1} becomes possible or the $(02^{0}0)-(01^{1}0)$ transition in the $\lambda = 16$ micron region.

Figure 2 shows the relations for the vibrational inverse population and the amplification index on the (03^{1}0)-(100) transition as a function of the braking temperature T_H. The values of ΔN and α in this case correspond to the fixed gas temperature in the jet $T = 100°$ K. The tendency toward a decrease occurring for $T_H \sim 1,600-2,000°$ K is characteristic for both relations. This tendency is connected with an increase in the VT-relaxation rate of the energy of the symmetric vibrations and also with the population of highly stimulated vibrational states progressing with an increase in the braking temperature.
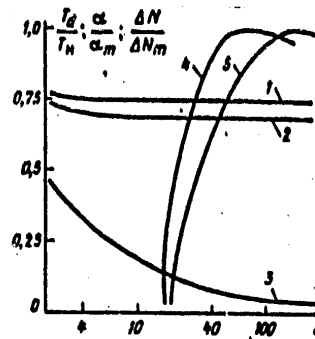
Figure 1. Distributions of the relative temperatures T_{12}/T_H (1), T_3/T_H (2), T/T_H (3), the inverse population $\Delta N/N_m$ (4) and the amplification index α/α_m (5) along the axis of the jet. The mixture of CO_2:A = 1:1, the initial pressure p_H = 10 atmospheres, the braking temperature T_H = 1,300° K; ΔN_m = 0.68 · 10^{16} cm^{-3}, α_m = 0.1 cm^{-1}.
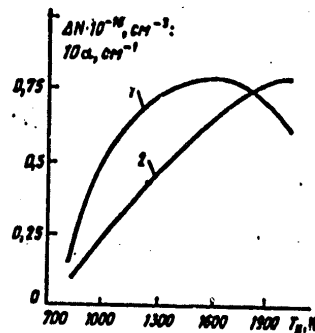

Figure 2. ΔN (1) and α (2) as functions of the braking temperature T_H for a mixture of CO_2:Ar = 1:1 for an initial density of the mixture ρ_H = 0.72 · 10^{20} cm^{-3}.

39

FOR OFFICIAL USE ONLY

In conclusion let us estimate the possible efficiency of a gas-dynamic CO_2-laser η on the transitions between twin mode levels. Considering that the generation of the laser emission is characterized in this case by the quantum efficiency equal to 1 and that it is possible only under the condition (1), we obtain

$$\eta = \varkappa \hbar \omega_2 \Delta l_{12}/(c_p T_M); \quad \Delta l_{12} = l_{12} - (l_{12})^*,$$

where c_p is the specific heat capacity of the gas mixture heated to the temperature T_H at constant pressure; χ is the proportion of the carbon dioxide molecules in the mixture. The value of $(l_{12})^*$ for $(T_{12})^* = 5T$ defines the flow rate of the nonequilibrium quantum reserve Δl_{12} of the symmetric vibrations admissible by the $(03^10)-(100)$ transition. From the data in Figure 2 it follows that the efficiency of the gas-dynamic CO_2-laser on this transition can reach values of $\eta \sim 5$ and 12 percent for braking temperatures of $T_H \sim 800$ and $1,500°$ K, respectively. Values of η that are just as high (by comparison with the ordinary type CO_2 gas-dynamic laser operating on the $(001)-(100)$ transition with $\lambda = 10.6$ microns) are caused by low energy of the vibrational quantum ($\hbar \omega_2 = 960°$ K) and the high specific heat capacity of the symmetric vibrations of CO_2. From this point of view the use of the gas-dynamic thermal pumping appears to be highly prospective for generation of laser emission on the CO_2 twin mode levels.

BIBLIOGRAPHY

1. A. A. Likal'ter, PRIKLADNAYA MEKHANIKA I TEKHNICHESKAYA FIZIKA, No 3, 1975, p 8.

2. A. A. Likal'ter, KVANTOVAYA ELEKTRONIKA, No 2, 1975, p 2399.

3. A. S. Biryukov and B. F. Gordiyets, PRIKLADNAYA MEKHANIKA I TEKHNICHES-KAYA FIZIKA, No 6, 1972, p 29.

4. Ye. M. Kudryavtsev and V. N. Fayzulayev, PRIKLADNAYA MEKHANIKA I TEKH-NICHESKAYA FIZIKA, No 6, 1973, p 25.

5. B. F. Gordiyets, A. I. Osipov, Ye. V. Stupochenko and L. A. Shelepin, UFN, No 108, 1972, p 655.

10845
CSO: 8144/0821-22

FOR OFFICIAL USE ONLY

UDC 535.375

EFFECT OF THE DEGREE OF POLARIZATION ON THE GAIN IN THE PRESENCE OF STIMU-
LATED RAMAN SCATTERING

[Article by A. Z. Grasyuk, V. N. Grebenyuk, V. F. Yefimkov, V. M. Izgorodin,
S. B. Kormer and K. B. Yushko; submitted 9 June 1978]

[Text] The basic factors defining the gain parameter in the presence of
stimulated Raman scattering as a function of the polarization state of the
stimulating radiation are the dependence of the spontaneous Raman scattering
cross section on the polarization of the incident light, the degree of de-
polarization of the stimulated scattering and the dependence of the square
of the electric field intensity of the incident light averaged over the os-
cillation period on the polarization state.

It is known that the Raman scattering cross section is determined by the de-
rivatives with respect to the coordinate of the isotropic and symmetric
parts of the polarizability tensor [1]. The intensities of the scattered
light are presented in relative units in Table [2] for certain combinations
of directions of the vectors E, k and k' (E is the electric field intensity
of the stimulating light, k and k' are the wave vectors of the incident and
scattered radiation). It is obvious that the scattering cross section does
not depend on the polarization state except when $k||k'$ (longitudinal pump-
ing).

In the presence of stimulated Raman scattering the depolarization leads to
the interaction of the pumping and the scattered radiation with the mutually
perpendicular directions of the vectors E and E' (E' is the electric field
intensity of the scattered light). It is possible to show that for the ex-
ponential mode of the gain of the Stokes component of the stimulated Raman
scattering, the degree of its depolarization is defined by the expression

$$\mathscr{P} = \rho \exp\left[-(1-\rho)\, g l_H\right].$$

where ρ is the degree of depolarization of the spontaneous scattering; g is
the gain in the presence of stimulated Raman scattering; I_H is the intensity
of the pumping radiation; l is the length of the nonlinear medium. If $\mathscr{P}$ is

41

FOR OFFICIAL USE ONLY

small, then the polarization of the incident and scattered light in practice coincide. Usually this case is realized [3].

Type of Scattering		Nonpolarized Light	Linearly Polarized Light	
Longitudinal	Scalar	3/2	3/2	
	Symmetric	21/20	21/20	
Transverse	Scalar	3/4	3/2	
	Symmetric	39/40	21/20	
Transverse	Scalar	3/4	0	
	Symmetric	39/40	9/10	

Since the nonpolarized light [4] can be represented in the form of the sum of two independent waves with mutually perpendicular directions of polarization and with an intensity equal to half the intensity of the initial light, for the longitudinal pumping and $\mathscr{P} \approx 0$ the threshold intensity for the nonpolarized light must be twice as large as for the linearly polarized light (see also [5]).
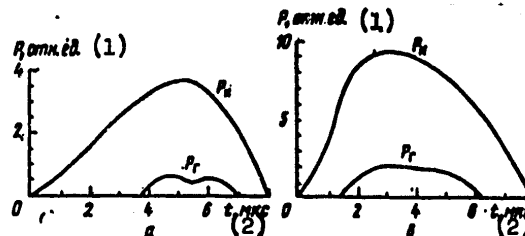
Pumping radiation power P_H and generation power P_Γ as functions of time for linearly polarized (a) and nonpolarized (b) light.

Key: 1. Relative units   2. Microseconds

In this paper the results are presented for measuring the threshold intensities of linearly polarized and nonpolarized pumping radiation for a liquid oxygen combination laser similar to the one described in [6, 7]. For it $\rho = 0.11$ [8] and for $I_{H1} = 3 \cdot 10^2$ MW/cm, $\mathscr{P} = 0.02$.

42

FOR OFFICIAL USE ONLY

FOR OFFICIAL USE ONLY

A photodissociation laser (wavelength 1.315 microns [9-11]) was used as the source, the emission of which was directed by a lens into the active medium placed in a resonator with plane-parallel mirrors. In order to decrease the effect of the generation development time on the determination of the threshold intensity, experiments with polarized and nonpolarized pumping were performed for the shortest possible length of the resonator.

The degree of polarization was determined by measuring the energy of the light beams reflected from the plates arranged in two mutually perpendicular directions at the Brewster angle. For polarized emission it was ≥ 0.98, and for nonpolarized emission, ~ 0. By the threshold intensity of the pumping we mean the value of $I = P_H/S$ (P_H is the threshold power; S is the area of the transverse cross section of the pumping beam averaged over the length of the active medium). The power $P_H = (1/2)(P_1 + P_2)$ (P_1 and P_2 are the values of the power at the time of occurrence and cessation of generation) was taken as the threshold power. Relations are presented in the figure for the pumping power and the first Stokes component as a function of time for linearly polarized and nonpolarized emission.

The measured values of the threshold intensities are 2.7 ± 1.3 and 5.2 ± 2.6 MW/cm^2 for linearly polarized and nonpolarized light. This corresponds to a gain of $(6.3\pm3.1) \cdot 10^{-3}$ and $(3.3\pm1.6) \cdot 10^{-3}$ cm/MW, and it agrees with the measurements taken in [8] (considering the variation of the wavelength). In the first case the values of the threshold intensity are 1.9 ± 0.2 times smaller than in the second case.

BIBLIOGRAPHY

1. I. Brandmueller and O. Moser, "Vvedeniye v spektroskopnyu kombinatsion-nogo rasseyaniya sveta" [Introduction to the Spectroscopy of Raman Scattering of Light], Moscow, Mir, 1964.

2. L. D. Landau and Ye. M. Lifshits, "Elektrodinamika sploshnykh sred" [Electrodynamics of Continuous Media], Moscow, Nauka, 1964.

3. P. D. Maker and R. W. Terhune, PHYS. REV., No 137, 1965, p A-801.

4. M. Born and E. Vol'f, "Osnovy optiki" [Fundamentals of Optics], Moscow, Nauka, 1970.

5. I. M. Bel'dyugin and Ye. M. Zemskov, KVANTOVAYA ELEKTRONIKA, No 4, 1977, p 1114.

6. A. Z. Grasyuk, V. F. Yefimov, I. G. Zubarev, V. I. Mishin and V. G. Smirnov, PIS'MA V ZhETF, No 8, 1968, p 474.

7. V. M. Izgorodin, S. B. Kormer and K. B. Yushko, "Tezisy dokl. na I Vsesoyuz. konf. 'Optika lazerov'" [Topics of Reports at the First All-Union Conference on Laser Optics], Leningrad, 1977.

FOR OFFICIAL USE ONLY

8. J. B. Grun, A. K. McQuillan and B. P. Stoicheff, PHYS. REV., No 180, 1969, p 61.

9. V. V. Kasper and G. S. Pimental, APPL. PHYS. LETTS, No 5, 1964, p 231.

10. A. J. De Maria and C. J. Ultee, APPL. PHYS. LETTS, No 9, 1966, p 67.

11. G. A. Kirillov, S. B. Kormer, G. G. Kochemasov, S. M. Kulikov, V. M. Murugov, V. D. Nikolayev, S. A. Sukharev and V. D. Urlin, KVANTOVAYA ELEKTRONIKA, No 2, 1975, p 666.

10845
CSO: 8144/0821-22

FOR OFFICIAL USE ONLY

SYNCHRONIZATION OF PLASMA-MIRROR ELECTROIONIZATION CO_2 LASERS

[Article by N. G. Basov, V. A. Boyko, V. A. Danilychev, V. D. Zvorykin,
A. N. Lobanov, I. V. Kholin and A. Yu. Chugunov, Physics Institute imeni
P. N. Lebedev of the USSR Academy of Sciences, Moscow; submitted 21 June
1978]

[Text] In [1] a new approach was proposed to the creation of laser devices
for spherically symmetric compression of thermonuclear targets. The essence
of this approach consists in using a plasma formed under the effect of laser
emission on the surface of the target as the common mirror of powerful elec-
troionization CO_2 lasers arranged uniformly over the sphere. The advantages
of the proposed system over the traditional laser systems using the princi-
ple of series-parallel amplification of a weak signal must include the ab-
sence of a master oscillator and the preliminary amplification stages with
optical decouplings for conversion of the self-stimulation of the device.
The self-consistent operating mode of a plasma-mirror laser makes it possi-
ble to ensure high spatial uniformity of irradiation of the target and it
lowers the requirements on the precision of adjustment of the optical ele-
ments.

The calculations of the laser initiation of a thermonuclear reaction in non-
uniform spherical targets [2] indicates that for an energy of the laser
emission of ~ 1 MJoule, target sizes of ~ 1 cm and laser pulse time parameters
characteristic of the plasma-mirror electroionization CO_2 laser (~ 100 nano-
seconds) [3], it is possible to obtain a gain with respect to energy of $\sim 10^3$.
The same calculations demonstrated the low sensitivity of the gain to the
wavelength of the heating radiation and the shape of the laser pulse. How-
ever, very high requirements are imposed on the symmetry of the irradiation
of the target.

This paper is on the problem of achieving the time synchronization of the
operation of several lasers required for symmetry of irradiation. Let us
note that the exact synchronization of the lasers cannot be ensured by sta-
bilization of only the electrical parameters of the devics. Even in the
case of strictly simultaneous inclusion of the laser pumping the random

45

FOR OFFICIAL USE ONLY

FOR OFFICIAL USE ONLY

small fluctuations of the pumping level, the composition of the operating mixture, optical Q-factor of the resonators, and so on lead to significant dispersion in time of the development of the generation pulses. In this paper methods are proposed for precise synchronization based on the introduction of an optical coupling between the laser resonators.

Synchronization of Two Lasers by a Common Target. A diagram of the experimental setup is presented in Figure 1a. The laser resonators were formed by plane mirrors 1, 2, spherical mirrors 4, 5 and a common target 6 located in a vacuum chamber. The active element of the two lasers was the 10-liter electroionization laser couvette 3 described in detail in [4] with an aperture of 10 x 10 cm. The diameter of each laser beam was determined by the diameter of the holes in the diaphragms 7, and it amounted to 2.5 cm. The distance between the optical axes of the resonators was 7 cm. Part of the laser emission was picked up from the resonators by light-separating plates of NaCl 8, 9 for the power detectors 10, 11. The signals from the detectors were amplified by two identical amplifiers, and they were fed through cables of equal length to one of the twin-beam tubes of the 6LOR-M oscillograph. The time parameters of the recording channels made it possible to measure the difference in times of the development of generation $\Delta\tau$ with a precision of ± 5 nanoseconds.
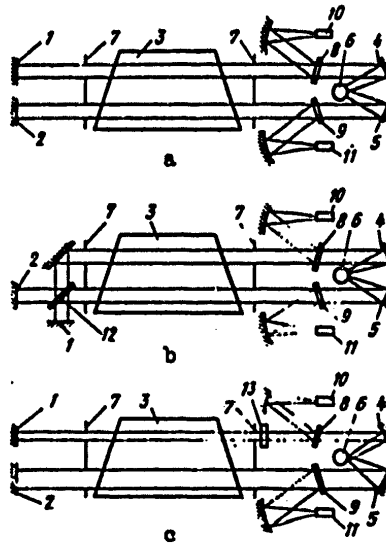

Figure 1. Optical systems of the experiments in laser synchronization.

When using one target as a common mirror for two lasers part of the radiation of each laser was reflected on the aperture of the focusing mirror of the other laser as a result of the diffuse [5] nature of the reflection of a ~100 nanosecond pulse from the plasma formed by the radiation on the surface of the target. This provided an optical coupling between the resonators.

46

FOR OFFICIAL USE ONLY

The dependence of $\Delta\tau$ at the 0.1 level of intensity of the laser signals on the distance l between the centers of the spots where the radiation was focused on the target was measured in the experiment. The results of the measurements for spot diameters of ~2 mm are presented in Figure 2. For l > 4 mm the optical coupling of the resonators was small, and the difference in times of development of generation reached $\Delta\tau$ ~ 300 nanoseconds. A decrease in l led to an increase in the optical coupling and corresponding sharp decrease in $\Delta\tau$. In the case of partial or complete overlap of the focusing spots (l < 2 mm) within the limits of accuracy of the measurements, complete synchronization of the operation of the lasers was observed.

Synchronization Using a Light-Separating Plate. The diagram of the experimental setup is presented in Figure 1b. Without the light-separating plate 12 the laser resonators were not optically coupled to each other (the radiation of the lasers was focused on the target in such a way that the focusing spots do not overlap). In this case, as a result of incomplete identicalness of the laser resonators, the difference in times of development of generation amounted to $\Delta\tau$ ~ 200-300 nanoseconds (see Figure 3a).

With the light-separating plane-parallel germanium plate installed, the reflection and the transmission coefficients of which were close to 50 percent, the radiation of each laser propagated from the target was separated by the plate into two beams and was mixed with two beams of the other laser. As a result of this "mixing" complete synchronization of the laser signals was achieved (Figure 3b).
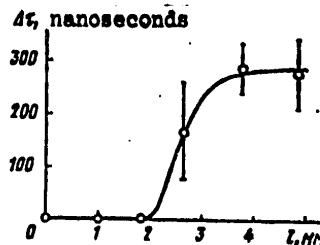

Figure 2. Difference in generation development times of two lasers $\Delta\tau$ as a function of the distance l between the centers of the spots where the radiation is focused on the target.

The proposed procedure can be applied for synchronization of four lasers using four light-separating plates. For synchronization of more than four lasers, the system for mixing the laser beams becomes extremely awkward for practical implementation, and the methods of solving the problem obviously must be found in a combination of the above-investigated synchronization techniques.

Control of Plasma-Mirror Lasers. The inclusion of the generation in a system of synchronized lasers at a given point in time can be ensured by external control of the coefficient of reflection of the emission from the target.

47

FOR OFFICIAL USE ONLY

A simple experiment demonstrates one of the methods of modulating the re-
flection coefficient using the radiation pulse of an additional controlling
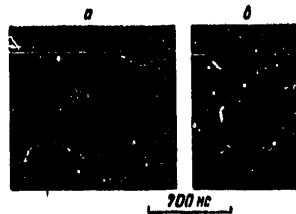laser forming a plasma on the surface of the target.

Figure 3. Oscillograms of nonsynchronized (a) and synchronized (b) genera-
           tion pulses of two lasers.

The diagram of the experimental setup is presented in Figure 1c. The reso-
nance of the lower laser in the diagram was formed by a plane mirror 2 and
the target 6 at the focal point of the mirror 5. The diameter of the laser
beam was 5 cm. The upper controlling laser on the diagram with beam diame-
ter of 2 cm operated with a common semitransparent mirror 13.

When using an organic glass target with a diffusely reflecting surface to
the formation of a plasma in the aperture of the focusing mirror 5 no more
than 0.1 percent of the incident radiation was scattered, and the laser res-
onator was characterized by a very high threshold of occurrence of genera-
tion. The pumping level for a closed beam of the controlling laser was es-
tablished somewhat below this threshold.

For an open generation beam of the controlling laser it led to the occurrence
of a plasma on the surface of the target and to an increase in the reflection
coefficient by approximately 10 times. The increase in positive feedback in
the resonator of the plasma-mirror laser, in turn, caused generation of it.
The time delay of the generation pulse with respect to the controlling laser
pulse was ~150 nanoseconds. The accuracy of inclusion of the plasma-mirror
laser was no worse than ±25 nanoseconds.

BIBLIOGRAPHY

1. N. G. Basov, I. A. Berezhnoy, V. A. Boyko, V. A. Danilychev, V. D.
    Zvorykin, V. V. Ignat'yev, I. V. Kholin and A. Yu. Chugunov, PIS'MA V
    ZhTF, No 1, 1975, p 1105.

2. Yu. V. Afanas'yev, N. G. Basov, P. P. Volosevich, Ye. G. Gamaliy, O. N.
    Krokhin, S. P. Kurdyumov, Ye. I. Levanov, V. B. Rozanov, A. A. Samarskiy
    and A. N. Tikhonov, PIS'MA V ZhETF, No 21, 1975, p 150.

FOR OFFICIAL USE ONLY

FOR OFFICIAL USE ONLY

3. N. G. Basov, V. A. Boyko, V. A. Danilychev, V. D. Zvorykin, A. N. Lo-
    banov, A. F. Suchkov, I. V. Kholin and A. Yu. Chugunov, KVANTOVAYA
    ELEKTRONIKA, No 4, 1977, p 1761.

4. I. A. Berezhnoy, V. A. Boyko, V. A. Danilychev, V. D. Zvorykin, V. V.
    Ignat'yev, I. V. Kholin and A. Yu. Chugunov, PTE, No 5, 1977, p 172.

5. N. G. Basov, V. A. Boyko, V. A. Danilychev, V. D. Zvorykin, I. V. Kho-
    lin and A. Yu. Chugunov, KVANTOVAYA ELEKTRONIKA, No 4, 1977, p 2268.

10845
CSO: 8144/0821-22

FOR OFFICIAL USE ONLY

FREQUENCY TUNING IN A DYE LASER WITH A BRAGG MIRROR UTILIZING A CHOLESTERIC LIQUID CRYSTAL

[Article by I. P. Il'chishin, Ye. A. Tikhonov, V. G. Tishchenko and M. T. Shpak, Physics Institute of the Ukrainian SSR Academy of Sciences, Kiev; submitted 27 June 1978]

[Text] 1. The interest in studies of liquid crystals in quantum electronics and nonlinear optics arises, in particular, from the possibility of continuous control of the optical characteristics by the superposition of weak external effects. The capacity of liquid crystals to change their texture easily permits small film-type elements which control and convert laser emission on the basis of them. Thus, thin layers of liquid crystals of the cholesteric type (LCC) were used for generation of the third harmonic [1, 2]. The introduction of generating organic dyes into oriented layers of nematic liquid crystals has made it possible to build lasers which change intensity, generation threshold, radiation pattern of the emission and polarization on reorientation of the liquid crystal layer [3, 4].

In this paper a report is presented on obtaining a frequency controllable dye laser, one of the resonator mirrors of which is an oriented LCC layer. A study was made of the variation of the generation frequency during thermal variation of the pitch of the LCC helix.

2. An oriented thin LCC layer with the helix axis normal to the bounding substrates is a medium, the dielectric constant of which is modulated with a period of $P/2 = \pi/q_0$, where P is the pitch of the cholesteric helix, q_0 is the angle of twist of the structure per unit length. A parallel beam of nonmonochromatic light incident at the angle θ on this structure will undergo coherent reflection on the λ which satisfies the Bragg condition $P \cos \theta = m\lambda_0$. Here λ_0 is the wavelength in the medium equal to λ/n, n = $(n_0 + n_e)/2$ is the mean index of refraction of the LCC.

The selectively reflected light has circular polarization, the form of which is given by the direction of twist of the cholesteric helix in an oriented flat texture. For normal incidence and sufficiently large number of helix

50

FOR OFFICIAL USE ONLY

windings in the LCC layer, the incident radiation of circular polarization is completely reflected in the first order [5], and the Bragg condition has form $Pn = \lambda$.

It is obvious that the wavelength of the selectively reflected light is determined by the pitch of the cholesteric helix which depends on the composition of the LCC, the temperature, the electric and magnetic fields and other disturbances [6-8].

3. In the experiment temperature adjustment of the pitch of the helix was used for normal orientation of the LCC layer with respect to the resonator axis. A tricomponent mixture of cholesterol chloride + cholesterol oleate + cholesterol nonanoate was used as the LCC in a gravimetric ratio of 1:1.33:1 at a temperature of 22° C approximately in the center of the temperature range of existence of the liquid crystal state. For this mixture the pitch of the helix increases monotonically with temperature $(dP/dT > 0)$. The LCC was placed in a cell formed by two glass plates. The thickness of the LCC layer was given by teflon inserts. The inside walls of the cell were covered by a transparent layer of SnO_2 and they were polished by the Chatelain method [9]. In order to obtain a uniform flat texture, the LCC layer was heated above the phase transition point to the isotropic state; then it was cooled slowly. At the phase transition temperature the plates were shifted in opposite directions by the method of [10] with subsequent slow cooling to room temperature.
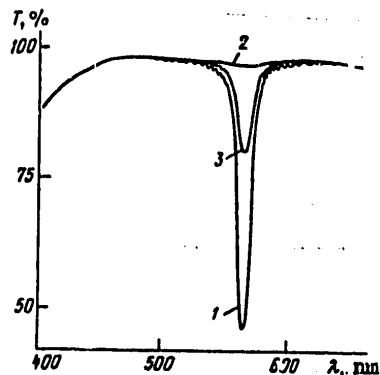

Figure 1. Selective transmission of an LCC layer (d = 15 microns) for lefthand (1) and righthand circularly polarized light (2) and also for linear polarization (3).

The selective transmission characteristics of the flat texture for different polarizations of the incident radiation are presented in Figure 1. The oriented LCC layer 15 microns thick reflects the lefthand circularly polarized radiation in the half-width band of $\Delta\lambda = 11$ nm with an efficiency of R = 52 percent. The temperature dependence of λ_{max} of the selective reflection for

FOR OFFICIAL USE ONLY

this LCC mixture is presented in Figure 2. The selective reflection wavelength varies linearly with variation of the temperature with a rate of 3.1 nm/deg. Near the phase transition temperature (39° C) the linear growth of λ_{max} with temperature ceases as a result of complete untwisting of the cholesteric helix. The variation of the reflection efficiency in the investigated temperature range as a result of dispersion of the plate used to obtain the circular polarization $\lambda/4$ did not exceed 5 percent.
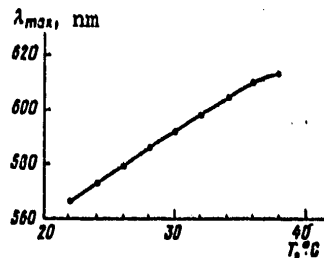
Figure 2. Temperature dependence of the selective reflection for the indicated LCC mixture (d = 15 microns).

The pumping source of the dye laser was the second harmonic radiation of the Nd^{3+} glass laser. A solution of rhodamine 6G in dimethylsulfoxide with an optical density of D = 7 at λ = 530 nm was used in the dye laser. The exit mirror of the resonator was a mirror with dielectric coatings and reflection in the size 560-620 nm range of R = 30 percent. The angle between the pumping radiation and the generation radiation of the dye laser was 7°. A couvette with the dye 10 mm thick was placed at the Brewster angle to the axis of the resonator. The cell with the LCC was placed in a thermostated holder, the thermal stabilization of which was no worse than 0.1° C. In order to improve the efficiency of the reflection, a phase plate was introduced into the resonator with a phase shift of $\pi/2$ for the tuning range. In this case linearly polarized generation emission was propagated in the resonator which was converted to lefthand circularly polarized immediately before the LCC. The pumping beam aperture was limited by a diaphragm 1 mm in diameter.

4. The experimental results are presented in Figure 3. Figure 3a shows the generation spectra of the dye laser in the temperature range of 22-28° C. The radiation was adjusted from 567 to 585 nm. The total width of the tunable frequency band reached 3.5 nm for pumping approximately 30 times the threshold value.

Two intense bands were observed in the generation spectra against the background of the wide tunable band. The spacing between the two intense bands was 2 nm. With a decrease in the resonator base from 300 to 150 mm (Figure 3b) and the same amount over the threshold, the generation took place in two narrow bands, the spacing between which was 2 nm. The band widths were 0.5

52

FOR OFFICIAL USE ONLY

FOR OFFICIAL USE ONLY

and 0.7 nm, respectively. The presence of a continuous nontunable genera-
tion spectrum in Figure 3a is caused by reflection from a plane-parallel
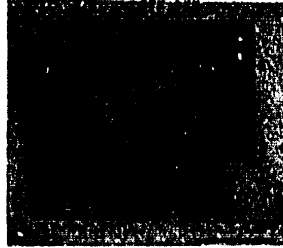cell with LCC and the $\lambda/4$ plate.

Figure 3. Generation frequency control of the dye on variation of the tem-
perature from 22 to 28° C (from bottom to top, resonator base
300 mm, a) and dye generation spectrum at a temperature of 23° C
(resonator base 150 mm, b).

The frequency tuning rate of the laser obtained with a precision of 0.1 nm
corresponds to the tuning rate observed for the temperature variation λ_{max}
of selective reflection, and it is determined by the thermal stabilization
error. The presence of two intense bands in a wide generation spectrum and
also the splitting of the wide band into two lines can be caused primarily
by nonuniformity of orientation of the LCC film both respect to area and
with respect to thickness. The proposed physical causes of this phenomenon
for the LCC with strong dependence of P on T were discussed in [10] where
the splitting of the selective reflection band was also obtained.

5. The performed investigation demonstrates the possibility of the applica-
tion of the oriented LCC layers for the selection and tuning of the fre-
quency of dye lasers. They can be used in lasers with sufficiently high
power for pulse durations where disordering of the structure of the LCC has
still not taken place. The rupture threshold of the LCC film by nanosecond
pulses is comparable with the rupture threshold of the transparent orienting
substrates. The use of LCC mixtures with a pitch which depends on the elec-
tric field [11] is prospective for the practical realization of the genera-
tion frequency tuning.

BIBLIOGRAPHY

1. J. W. Shelton and Y. R. Shen, PHYS. REV. LETTS, No 26, 1971, p 538.

2. S. A. Akopyan, S. M. Arakelyan, R. V. Kochikyan, S. Ts. Nersisyan and
   Yu. S. Chilingaryan, KVANTOVAYA ELEKTRONIKA, No 4, 1977, p 1441.

53

FOR OFFICIAL USE ONLY

3. I. P. Il'chishin, Ye. A. Tikhonov, M. T. Shpak and A. A. Doroshkin, PIS'MA V ZhETF, No 24, 1976, p 336.

4. E. Tikhonov, M. Bertolotti and F. Scudieri, APPL. PHYS., No 11, 1976, p 357.

5. H. De Vries, ACTA CRYSTALLOG., No 4, 1951, p 219.

6. R. D. Ennulat, MOL. CRYST. LIQ. CRYST., No 13, 1971, p 337.

7. F. J. Kahn, PHYS. REV. LETTS, No 24, 1970, p 209.

8. L. M. Blinov, S. V. Belyaev and V. A. Kizel, PHYSICS LETTS, No 65A, 1978, p 33.

9. P. Chatelain, BULL. SOC. FRANS. MINERAL, No 66, 1943, p 105.

10. V. A. Kizel' and S. I. Kudashev, ZhETF, No 72, 1977, p 2180.

11. E. Spitz and D. Ostrowsky, FRANS. PAT., No 2, 1973, pp 137, 166.

10845
CSO: 8144/0821-22

FOR OFFICIAL USE ONLY

GENERATION OF HIGH-POWER ULTRASHORT PULSES BY A LOW-TEMPERATURE RUBY LASER
WITH SMALL VOLUME OF THE ACTIVE MEDIUM

[Article by A. N. Kirkin, A. M. Leontovich and A. M. Mozharovskiy, Physics
Institute imeni P. N. Lebedev of the USSR Academy of Sciences, Moscow; sub-
mitted 1 March 1978, revised 1 July 1978]

[Text] A self-mode-locked low-temperature ruby laser can generate a short
train of 1-3 pulses [1]. This is caused by the fact that at low temperature
a ruby has a large operating transition cross section, and the amplification
coefficient of the active medium can reach a value on the order of 1 cm^{-1} at
the time of illumination of the saturable filter when using filters with
initial transmission of about 1 percent. The energy stored in the medium is
released in this case in a small number of passes of the light in the reso-
nator.

In [2] a study was made of the time characteristics of the ruby laser emis-
sion using an image converter with time scanning. The emission was in the
form of a short train of pulses with an energy of 0.02 joules and a duration
of 35 picoseconds. This duration is less than the transverse relaxation
time of the ruby at the temperature of nitrogen (on the order of 100 pico-
seconds [3]), and the interaction of the radiation with the material can oc-
cur coherently in this case [4, 5]. For coherent interaction of the light
pulse with the amplifying medium, its "area"

$$\theta = d/\hbar \int_{-\infty}^{\infty} E(t)dt$$

(E is the light field amplitude, d is the matrix dipole moment of the tran-
sition) approaches a steady-state value of π as it is propagated, the maxi-
mum amplitude increases, and the shape and duration change. In [6, 7] a
study was made of self-induced transparency and coherent amplification in a
ruby at the temperature of liquid nitrogen. It was demonstrated that gener-
ation of a π-pulse can take place in a ruby laser. In the case of coherent
amplification, the pulse duration is shortened by up to two times (from 35
to 18 picoseconds).

55
FOR OFFICIAL USE ONLY

In this paper the characteristics of the ruby at low temperature (the possibility of generation of a short train under self-mode-locking conditions and shortening of the pulse with coherent amplification) have been used in practice to obtain high-power (duration 10 picoseconds, energy 1 joule) ultrashort pulses with small volume of the active medium. A study was made of the relation between the pulse duration and the radiation line width in the amplification process. A high-speed optical shutter was proposed and used to measure the pulse duration.
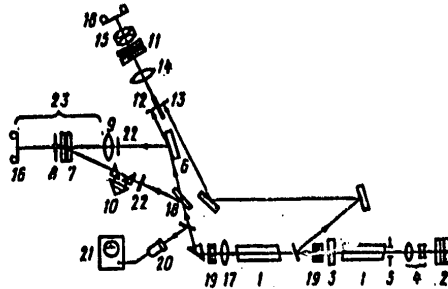
Figure 1. Diagram of the experimental setup: 1—ruby crystals; 2—mirror (R = 100 percent) with couvette; 3—wedge substrate (R = 4 percent); 4—telescope; 5—diaphragm 6 mm in diameter; 6—echelette grating; 7—couvette with saturable filter; 8—diaphragm 1 mm in diameter at the focal point of the lens 9; 10—delay line; 11—Fabry-Perot interferometer; 12—diaphragm; 13—scatterer; 14—lens; 15—objective; 16—camera; 17—long focal length lens; 18—semitransparent mirror; 19—decoupling; 20—FEK 15 photoelement; 21—I2-7 oscillograph; 22—neutral light filter; 23—high-speed optical shutter.

The diagram of the experimental setup is presented in Figure 1. Ruby rods $\emptyset$ 12 x 120 mm with Cr^{3+} ion concentration of 0.05 percent were used in the generator and amplifier. They were cooled by nitrogen vapor to 100° K. The ends of the rods were cut at an angle of 6°. The resonator was formed by a 100-percent mirror in contact with the saturable filter and wedge substrate (R = 4 percent). A telescope with 1.8X magnification adjustable to a negative region was placed between the saturable filter and the end of the illuminator. This created an unstable resonator configuration, and it made it possible to increase the generation energy with stable mode synchronization as a result of increasing the beam diameter to 6 mm. The generation energy exceeded by an order the energy obtained in [2], and it reached 0.2 joule for an energy flux of 1-2 joules/cm^2. The divergence of the radiation was corrected by a long-focus lens placed at the output of the amplifier. The radiation energy was measured by an IZhK-1 calorimeter. A solution of cryptocyanin in nitrobenzene with initial transmission of 1-2 percent (couvette thickness of 2 mm) was used as the saturable filter. The self-mode locking was observed in a wide range of telescope adjustments.

56

The radiation energy reached 0.5 joule after amplification. The pulse duration at the output of the amplifier was measured by a high-speed optical shutter with saturable filter [7, 9]. With this measurement technique the pulse track obtained using a scatterer is photographed through a shutter, the opening time of which is less than or comparable to the pulse duration. In order to increase the shutter speed by comparison with [7, 9], an echelette (150 lines/mm) was used as the scatterer on which the beam was directed at the glancing angle. The fifth diffraction procedure was used for the experiment. The total length of the echelette corresponded to a duration of 45 nanoseconds. The high speed of the shutter made it possible to use a saturable filter with small initial transmission (10^{-6}) and to decrease the "closing time" of the shutter by comparison with the dye relaxation time. A solution of cryptocyanin in ethanol (couvette thickness 1 mm) was used as the saturable filter. As a result of the low initial transmission of the saturable filter, the recorded track corresponded to the pulse of the train with maximum amplitude; the closure time of the shutter was less than 1 picosecond by the estimates. The transmission of the saturable filter in the illuminated state was 10^{-2}. Considering the properties of the photographic film (type 15) the track contrast could reach 20. The finite opening time of the shutter could not lead to a difference of the recorded track length of more than two times from the actual length. The pulse duration at the output of the amplifier was estimated by the track length and it was 10-20 picoseconds at half the altitude. An example track is presented in Figure 2. An oscillogram is also presented there for the radiation at the amplifier output. The signal was recorded by the FEK-15 coaxial photoelement and the I2-7 oscillograph.

Figure 2. Oscillogram of radiation (a) and pulse track (b) at the output of the amplifier.

The spectral width of the radiation at the output of the amplifier was measured by a Fabry-Perot interferometer, and it was equal to 1.0-1.5 cm^{-1} at half the height. The interaction of the radiation with the material in the amplifier took place coherently. The effect of the self-induced transparency observed on transmission of the radiation of the amplifier through the unpumped ruby rod (analogous to the one used in the generator and the amplifier) is confirmation of this. The transmission of the sample for the 2π-pulse obtained by compression of the amplifier beam by two times was 0.1, and it coincided with the results of [6]. Here the radiation spectrum was not broadened. This indicates absence of significant nonlinear distortions of the pulse. The radiation spectrum of the generator and the amplifier was

photographed simultaneously on one frame. The edge of the diaphragm 12 used in the interferometer exposure system was placed at the focal point of the lens 14.

Figure 3. Radiation spectrum of the generator (right) and amplifier (left); region of dispersion of the Fabry-Perot interferometer 2.5 cm^{-1}.

The systematic broadening of the spectrum was recorded for amplification to 1.6 times (see Figure 3). It was caused by a reduction in the pulse duration during coherent amplification. The product $\Delta\nu \cdot \Delta t$ of the width of the amplifier spectrum times the pulse duration (taken at half-height) was 0.2-0.8. It must be considered that this value can be somewhat less than the corresponding value for a single pulse. This is caused by the fact that for coherent amplification in the case of absence of nonlinear distortions the maximum pulse out of the pulse train can have minimum duration. Therefore the spectral width of the entire train can be less than the spectral width of its maximum pulse.

With further amplification of the radiation by two such amplifiers, the energy increased to 1.0-1.2 joules, and the pulse duration was reduced to 5-10 picoseconds. Here the radiation spectrum was broadened to 2.0-2.5 cm^{-1}. The divergence of the radiation was measured using a mirror wedge [10], and it was $2 \cdot 10^{-3}$ (with respect to the half-energy level). During prolonged operation, the negative lens of the telescope in the resonator was damaged; the probability of mode synchronization was decreased in this case. In order to improve the stability of the operating conditions, the telescope in the resonator was replaced by a scattering lens with a focal length of 2-3 m. The results did not change significantly in this case. There were no volumetric disturbances in the ruby.

The authors express their appreciation to M. D. Galanin for his interest and attention to this work.

BIBLIOGRAPHY

1. A. M. Leontovich, Ye. D. Bayeva and A. M. Mozharovskiy, KVANTOVAYA ELEKTRONIKA, edited by N. G. Basov, No 4 (16), 1973, p 106.

2. A. M. Leontovich, A. M. Mozharovskiy, Yu. N. Serdyuchenko and M. Ya. Shchelev, KVANTOVAYA ELEKTRONIKA, No 1, 1974, p 691.

3. A. Shavlov, in the book "Lazery" [Lasers], Moscow, IL, 1963.

4. S. L. McCall and E. L. Hahn, PHYS. REV., No 183, 1969, p 457.

5. S. L. McCall and E. L. Hahn, PHYS. REV. A, No 2, 1970, p 861.

6. A. M. Leontovich and A. M. Mozharovskiy, PIS'MA V ZhETF, No 19, 1974, p 347.

7. A. M. Leontovich and A. M. Mozharovskiy, PIS'MA V ZhETF, No 20, 1974, p 664.

8. A. N. Zherikhin, V. A. Kovalenko, P. G. Kryukov, Yu. A. Matveyets, S. V. Chekalin and O. B. Shatbershvili, KVANTOVAYA ELEKTRONIKA, No 1, 1974, p 377.

9. G. Mourou, B. Drouin and M. Denariez-Roberge, APPL. PHYS. LETTS, No 20, 1972, p 453.

10. V. V. Ragul'skiy and F. S. Fayzullov, OPTIKA I SPEKTROSKOPIYA, No 27, 1969, p 707.

10845
CSO: 8144/0821-22

FOR OFFICIAL USE ONLY

UDC 621.378.33

STUDY OF A PULSED H_2-F_2 CHEMICAL LASER AT HIGH PRESSURES OF THE WORKING MEDIUM

Moscow KVANTOVAYA ELEKTRONIKA in Russian Vol 5, No 12, 1978 pp 2642-2645

[Article by Yu. A. Kolchin, V. B. Kolovskiy, S. Ya. Pshezhetskiy and N. F. Chebotarev; submitted 10 October 1977, revised 3 May 1978]

[Text] At this time the primary efforts of the researchers dealing with chemical laser systems have been aimed at setting the H_2-F_2 or $D_2-F_2-CO_2$ lasers having high specific parameters (energy output of about 150 joules/liter [1, 2]. Recently a significant number of experimental and theoretical papers have been published where H_2-F_2 chemical lasers have been analyzed (see, for example, [3-7]).

It is known that in order to obtain maximum efficiency, a powerful short initiation of the reaction is required, and in order to obtain high specific power it is necessary to use optimal pressure of the mixture which, generally speaking, can be higher than atmospheric.

Accordingly, the problem of studying H_2-F_2 lasers at increased pressure of the components and with powerful initiation has become an urgent one.

The H_2-F_2 laser with a pressure of the components to 1 atmosphere was studied in the papers [5, 7] in which a linear increase in the output energy of the laser was observed with an increase in pressure. A pressure above 1 atmosphere was used in [3] where a parametric analysis was made of such a laser, and the output energy was measured as a function of the pressure of the mixture within the limits of 0-3 atmospheres. The maximum energy output was obtained for a pressure of about 1 atmosphere. The theoretical calculations of the laser in a wide power range and wide range of initiation times, pressures of the mixture and its composition [6] demonstrated that depending on these quantities, the optimal pressure can significantly exceed atmospheric. The absence of a sufficient quantity of experimental data complicates comparison of the theoretical calculations with the experimental data.

The purpose of this paper was to trace the laws and the trends in the behavior of the output energy of a fluorine-hydrogen laser in the pressure range

of the components of 0-5 atmospheres with light initiation of different duration and power.

Experimental Procedure

An ordinary laser device with initiation of two times was used for the measurements: 1) the IFP-5000 xenon tube placed alongside a laser couvette and fed from a capacitor bank with a capacitance of 2.8 microfarads across an air gap; 2) a specially manufactured coaxial tube constituting a unit with the capacitor, the discharger and the laser couvette. The laser couvette with an active volume of 2.5 cm^3 was located inside the discharge gap. The discharger, the tube and the capacitor of this structural design are described in detail in [8]. The low inductance of the discharge circuit made it possible to obtain a pulse duration of 0.7 microsecond with a front of 250 nanoseconds. In the usual version of illumination, the pulse duration was 7 microseconds; the active volume was 14 cm^3. In both cases the resonator was formed by a blind mirror R = 3 m and an Al_2O_3 plate. The components were mixed in the dynamic mode, and the exchange of the mixture in the laser couvette took place in less than 1 second.

The formula for the initiation pulses obtained using the FEK-22-SPU and the S8-11 and the I-2-7 oscillograph is illustrated in Figure 1.

Figure 1. Shape of the light initiation pulses in the first (a) and in the second (b) version (the marks are made every 50 nanoseconds).

The intensity of the light flux was measured in this experiment using the indicated initiation procedures. In connection with the difficulty of determining the F atom concentration during photolysis the following procedure was developed which is based on determining the amount of ClF_3 formed during photolysis of ClF.

It is known that the absorption peaks of ClF and F_2 almost coincide (274 and 284 nm, respectively) [9, 10]. The optical absorption curves in this region have the same shape according to our measurements. The F_2 absorption cross section is approximately twice as large as the ClF absorption cross section. In this case, by determining the number of ClF molecules dissociating during photolysis, it is possible to calculate the number of decomposed F_2 molecules.

In [9] it was demonstrated that the following processes take place during photolysis of the ClF molecules:

$$ClF + h\nu \rightarrow Cl + F; \tag{1}$$

61

$$Cl + ClF \rightarrow Cl_2 + F; \tag{2}$$

$$F + ClF \rightarrow ClF_2; \tag{3}$$

$$F + ClF_2 \rightarrow ClF_3. \tag{4}$$

It follows from this that the quantum yield of ClF_3 during photolysis of ClF is equal to 1. Thus, measuring the amount of ClF_3, it is possible to obtain a number of absorbed quanta. The amount of ClF_3 was determined on the Specord device by variation of the optical density and the maximum absorption region of ClF_3 (208 nm). Instead of the operating mixture, for a pressure corresponding to the optically thin layer, ClF was let into the laser couvette. After several flashes of the light, the contents of the couvette were refrozen in a quartz optical couvette. The amount of formed ClF_3 and, therefore, the number of absorbed quanta were determined by the variation of the optical density on a wavelength of 208 nm.

The quantum flow in the ClF and the F_2 absorption region averaged over the wavelength amounted to $1.15 \cdot 10^{17}$ cm^{-2} in a pulse or $1.5 \cdot 10^{23}$ cm^{-2} sec^{-1} for a coaxial tube, and for an ordinary tube (the first version of initiation), $0.4 \cdot 10^{17}$ cm^{-2} in a pulse or $0.5 \cdot 10^{22}$ cm^{-2} sec^{-1}. The degree of dissociation of the ClF was equal to 0.04 percent for the first tube and 0.13 percent for the second tube in a pulse. For fluorine, these values are two times larger. The accuracy of determining the indicated values was 30-40 percent. The characteristic generation time in the case of the application of a coaxial tube was ~1 microsecond for a pressure of 1 atmosphere of a mixture of $F_2:H_2:O_2:He = 1:0.33:0.24:8$. The generation time was approximately inversely proportional to the pressure of the mixture. The fluorine dissociation takes place in this case during the entire time of the existence of generation. In the first version the generation time was significantly less than the initiation time and, correspondingly, the proportion of the dissociated fluorine in the generation time was less. This means that the initiation with respect to atomic fluorine in these two cases differs by more than an order of magnitude.

Results and Discussion

As is known [11], with an increase in pressure of the mixture, several competing processes take place. The growth of the rate of formation of HF* is prevented by the reactions of breaking the chain as a result of recombination of the F and H atoms in ternary collisions and the reaction $H + O_2 + M \rightarrow HO_2 + M$, and the break in generation is promoted by the VT-relaxation processes. At the same time, the increase in pressure as a result of introduction of inert additives into the mixture, equalizing the rotational temperature, can lead to an increase in the efficiency [4]. The optimal pressure of the mixture will be determined by the expression for the rates of the competing processes and it will depend on the composition of the mixture and the initiation power. The experimental results are presented in Figure 2 where the relations are shown for the specific energy as a function of

the pressure of the mixture, the degree of dilution of the mixture by helium
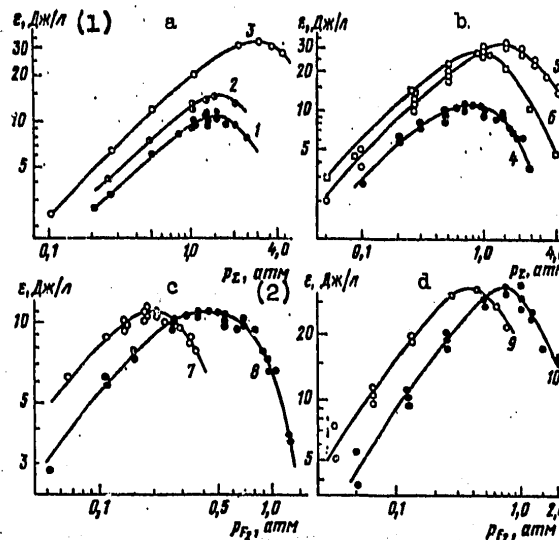and the initiation power.

Figure 2. Specific output energy as a function of the pressure of the mixture (a, b) and as a function of the partial pressure F_2 (c, d) for the following values of the parameters: composition of the mixture: $F_2:H_2:O_2:He:SF_6 = 1:0.3:0.2:6:0$ (1-3, 7, 9), 1:0.3:0.2:0.3:0 (4, 8), 1:0.3:0.5:0.3:0 (5), 1:0.3:0.5:0.3:0.33 (6); type I initiation (1, 2, 4, 7, 8), type II (3, 5, 6, 9, 10); U = 15 (1, 4, 7, 8), 19 (3, 5, 6, 9, 10), 20 kv (2).

Key: 1. Joules/liter   2. Atmospheres

Figure 2a shows the specific energy ε of the laser as a function of the pressure of the mixture $F_2:H_2:O_2:He = 1:0.3:0.2:6$ for different voltage on the feed capacitors in two versions of the initiation.

Figure 2b shows the dependence of ε on the pressure of the mixture in practice not diluted by helium ($He/F_2 = 0.3$). Figure 2a, b shows the effect of the initiation power on the dependence of ε on pressure. It is obvious from this that with an increase in the initiation power (that is, the degree of dissociation of F_2 in the generation time) with a simultaneous decrease in the pulse front not only ε increases, but the maximum of the specific energy as a function of pressure is shifted in the direction of higher pressures (from 1.5 to 3 atmospheres for mixtures diluted with helium and from 0.8 to 1.5 atmospheres for undiluted ones), whereas with an increase in the pulse energy without significant variation of its shape this is not observed (curves 1 and 2).

—

FOR OFFICIAL USE ONLY

Figure 2c, d shows the effect of the dilution of the mixture by helium on the dependence of ε on the fluorine pressure, that is, on the chemical efficiency. Curve 7 was obtained for $He/F_2 = 6$, curve 8 for $He/F_2 = 0.3$. In Figure 2c it is obvious that dilution of the mixture by helium leads to an increase in the chemical efficiency although the specific output energy does not increase here. This is obviously explained by the negative effect of the VT-relaxation processes and recombination of the active centers in the ternary collisions.

Figure 2b (curve 6) shows the effect of SF_6 ($SF_6/F_2 = 1/3$) on the specific energy output. Some increase in the energy output was observed in the pressure range to 1 atmosphere. With pressure the energy output decreased by comparison with the same mixture without SF_6.

The data obtained indicate a more complex effect of the initiation, the total pressure and the composition of the mixture on the output parameters of the fluorine-hydrogen laser with a pressure of the components above atmospheric and for lower pressures of the components. Increasing the intensity of the light initiation by more than an order leads to doubling of the specific energy of the emission. By comparison of the optimal pressures of the mixture obtained experimentally with those calculated [6] demonstrated good correspondence of them.

BIBLIOGRAPHY

1. N. G. Basov, A. S. Bashkin, P. G. Grigor'yev, A. I. Orayevskiy and O. Ye. Porodinkov, KVANTOVAYA ELEKTRONIKA, No 3, 1976, p 2067.

2. A. S. Bashkin, P. P. Grigor'yev, V. I. Igoshin, V. Yu. Nikitin and A. I. Orayevskiy, KVANTOVAYA ELEKTRONIKA, No 4, 1977, p 1004.

3. V. Ya. Agroskin, G. K. Vasil'yev, V. I. Kir'yanov and V. L. Tal'roze, KVANTOVAYA ELEKTRONIKA, No 3, 1976, p 1932.

4. G. K. Vasil'yev, V. I. Gur'yev and V. L. Tal'roze, ZhETF, No 72, 1977, p 943.

5. Hao-Lin Chem, R. L. Taylor, J. Wilson, P. Lewis and W. Fyfe, J. CHEM. PHYS., No 61, 1974, p 306.

6. V. I. Igoshin, V. Yu. Nikitin and A. N. Orayevskiy, KVANTOVAYA ELEKTRONIKA, No 4, 1977, p 1282.

7. D. B. Nickols, R. B. Hall and J. Doyle McClure, J. APPL. PHYS., No 47, 1976, p 4026.

8. Yu. A. Yanayt, Yu. M. Anisimov and V. I. Pchelkin, PTE, Vol 6, No 2, 1973, p 181.

FOR OFFICIAL USE ONLY

9. E. A. San Roman and H. J. Shumacher, Z. PHYS. CHEM. BD., No 71, 1970, p 153.

10. R. K. Steunenberg and R. C. Vogel, J. AMER. CHEM. SOC., No 78, 1961, p 901.

11. A. S. Bashkin, V. I. Igoshin et al., "Khimicneskiye lazery. Itogi nauki i tekhniki. Ser. Radiotekhnika" [Chemical Lasers. Science and Engineering Results. Radio Engineering Series], Vol 8, Moscow, VINITI AN SSSR, 1975.

10845
CSO: 8144/0821-22

FOR OFFICIAL USE ONLY

EFFECT OF PHOTOINITIATING MATERIALS ON THE GENERATION OF A PULSE TO HF
CHEMICAL LASER

[Article by Yu. I. Kozlov, N. Kh. Petrov, S. Ya. Pshezhetskiy and N. F.
Chebotarev; submitted 3 May 1978]

[Text] One of the methods of increasing the efficiency of chemical lasers
is the introduction of materials having a larger absorption cross section in
the spectral region of light pumping than the initial F_2 molecules [1, 2]
into the basic laser mixture. Multiatomic metal fluorides, inert gases or
halides, for example, MoF_6, VF_5, JF_7, ClF_5 and so on can serve as these
photoinitiating components. However, up to the present time the character-
istics of laser systems containing photoinitiating components, in particu-
lar, the possible negative effect of the photoinitiating components on the
generation parameters, have not been defined.

In this paper a study is made of the effect of some such photoinitiating ma-
terials on the output energy of laser generation in mixtures of F_2 and ClF
with H_2 having the greatest output parameters and efficiency [3].

Experimental Procedure

The experiment was performed on a device analogous to that described in [4,
5]. A quartz laser tube was used with an inside diameter of 17 mm and a
length of the active section of 70 cm. The ends of the tube were covered
by windows of CaF_2 installed at the Brewster angle. The photolysis of the
mixture was realized by a flash tube with xenon filling (p = 30 mm Hg). The
electric energy storage element was a capacitor bank, the structural design
of which made it possible to vary the capacitance in the range of 0-7.5 mi-
crofarads. The voltage on the bank had to be raised to 20 kv. The commut-
ing element in the discharge circuit was an air discharger which responds on
the approach of two copper balls 20 mm in diameter.

The experiments were performed for two different initiation powers: C = 1.5
microfarads, U = 13.5 kv, τ = 5 microseconds (1) and C = 7 microfarads, U =
20 kv, τ = 12 microseconds (2) (C is the capacitance of the bank of feed

66

FOR OFFICIAL USE ONLY

capacitors, U is the operating feed voltage, τ is the duration of the initiating light pulse measured on the $1/2$ maximum level). For each of the versions, the intensity of the light flux was measured in the ClF and F_2 absorption region. The procedure developed by the authors for measuring the light flux was based on determining the amount of ClF_3 formed during the photolysis of the ClF, and it was described in detail in [6]. The measurement showed that case (1) corresponds to the incident light flux $J_n = 10^{16}$ cm^{-2} for the pulse, and case (2) corresponds to $J_n = 4 \cdot 10^{17}$ cm^{-2} for the pulse. The accuracy of determining the indicated values is ± 50 percent.

The energy of the laser emission was measured by the KIM-1, IMO-2 and IKT-1M calorimeters. For preparation of the working mixtures, technical hydrogen and high-frequency helium were used. The hydrogen and helium were carefully dried by 5A zeolite; the ClF was synthesized at 300° C from an equimolar mixture of ClF_3 and Cl_2. Further removal of the F_2 was accomplished by evacuation at the temperature of liquid oxygen and removal of Cl_2, ClF_3, ClF_5, HF by redistillation in a vacuum at $t = -120^\circ$ C. The degree of purification was determined by the absorption spectra.

The admission and mixing of the gases were realized by a system of stainless steel needles. The addition of the gases to the laser tube was accomplished in the dynamic mode. Mixtures of nonreacting components at various pressures were made in 3-liter stainless steel mixing vessels. Then the vessels were connected to each other, and the mixtures were admitted to the operating volume through a common valve, mixing in the stream.

Results and Discussion

In [4] it was shown that the largest number of fluorine atoms during photolysis of the investigated fluorides by the pulse xenon tubes are formed from VF_5, and the least number, from WF_6. Beginning with this, a study was made of the effect of the VF_5 additives on the output energy of a laser based on F_2-H_2 and $ClF-H_2$ systems. Figure 1 shows the output energy of a laser based on a mixture of $ClF + H_2$ as a function of the VF_5 concentration for initiation powers corresponding to the cases (1) and (2). It is obvious that the effect of VF_5 essentially depends on the initiation power. In the case of "weak" initiation (1) 10 percent VF_5 (with respect to ClF) will lead to an increase in the output energy (consequently, to growth of the chemical and total efficiency) by 10-20 times depending on the fresher range and the tuning of the resonator (the output mirror for the measurements was an Al_2O_3 plate). In the case of "strong" initiation (2), the increase in output energy is observed only for pressures to 20 mm Hg. At higher pressure the addition of VF_5 leads to a decrease in the output energy.

The effect of the VF_5 additives (8.8 percent) on the H_2-F_2 and $ClF-H_2$ systems is illustrated in Figure 2. It is obvious that without the VF_5, the generation energy in the F_2-H_2 system under weak initiation conditions is 6-10 times higher than the energy on the $ClF-H_2$ system; on introduction of VF_5, both systems have equal output energies. The generation delay is measured under there conditions with respect to the beginning of initiation and

67

FOR OFFICIAL USE ONLY

also the generation duration were identical for both systems. Hence, it is possible to conclude that on introduction of the photoinitiating components and for low initiation pulse power, that is, when the initiation of the reaction is basically determined by the photodissociation of the photoinitiating component, the $ClF-H_2$ and the F_2-H_2 systems have close parameters. It must be noted that the VF_5-H_2 laser system has low efficiency and, consequently, the basic contribution to the laser emission is made by the $F_2 + H_2$ and the $ClF + H_2$ reactions. The relations for the output energy as a function of the total pressure of the mixture based on the VF_5-H_2 system for the initiations (1) and (2) are illustrated in Figure 3.
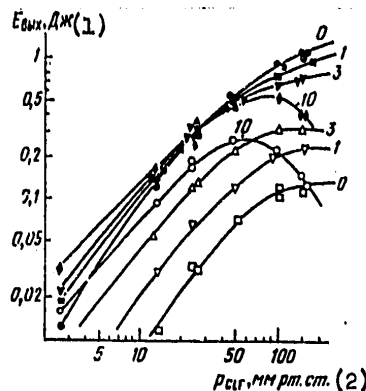
Figure 1. Output energy of a laser based on a mixture of $ClF:H_2:He:VF_5$ = 1:0.3:(1.7 - x):x as a function of the ClF pressure for different initiation powers and VF_5 concentrations. The numbers on the circles indicate the percentage of VF with respect to ClF; the light dots correspond to initiation 1), and the dark dots, initiation 2).

Key: 1. E_{out}, joules   2. mm Hg

In order to explain the different effect of the VF_5 (and, obviously, other photoinitiating components) for different intensity of the initiation, let us consider the output energy as a function of the initiation energy in the mixtures with VF_5 and without it in the $ClF-H_2$ system (see Figure 4). It is obvious that under the conditions of the specific experiment for pumping energy of 1.4 kilojoules, the addition of 10 percent VF_5 does not make any contribution to the generation energy, and with further growth of the pumping energy, the mixture with VF_5 additive gives less output energy than the "pure" mixture. The intersection of curves 1 and 2 in Figure 4 indicates the existence of a critical pumping power for which the output energies of the lasers based on the "pure" mixture and on the mixture with photoinitiating components are compared. On initiation less powerful than critical, the application of the photoinitiating component leads to a gain in output energy. For more powerful initiation the addition of the photoinitiating component leads to a reduction in the output energy.

68

FOR OFFICIAL USE ONLY

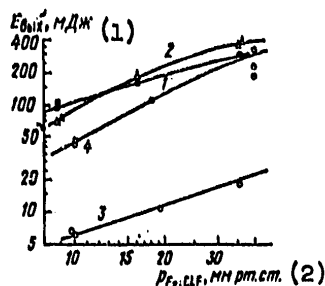Figure 2. Output energy of a laser based on mixtures of ClF-H_2 and F_2-H_2 as a function of the ClF and F_2 pressure with initiation (1): 1--mixture, ClF:H_2:He:VF_5 = 1:0.3:7.6:0.088; 2--mixture, F_2:H_2:He:O_2:VF_5 = 1:0.3:7.5:0.1:0.088; 3, 4-- mixtures 1, 2, respectively, without the VF_5 additives.
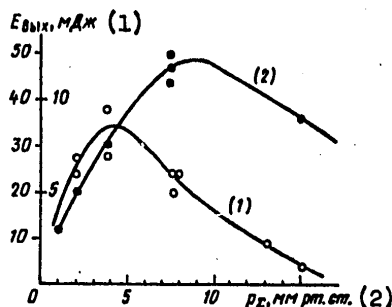
Key: 1. E_{out}, MJoules   2. mm Hg

Figure 3. Output energy of a laser based on a mixture of VF_5:H_2:He = 1:0.5:2.4 as a function of the total pressure of the mixture for the initiations (1) and (2): (1) right scale; (2) left.

Key: 1. E_{out}, MJoules   2. mm Hg

The negative role of the photoinitiating component in the F_2-H_2 laser is manifested for weaker initiation than in the ClF + H_2 laser. This is illustrated by the data in Figure 5 from which it follows that on initiation with a pumping energy of 1.4 kilojoules, the generation energy of the HF laser based on a mixture of F_2-H_2 with the addition of MoF_6 decreases by 50 percent.

The decrease in output power of the laser on addition of the photoinitiating component under powerful initiation conditions can be connected both with the relaxation on the molecules of the photoiniating component and the products of their photolysis, and with the participation of these particles in

69

FOR OFFICIAL USE ONLY

the separation reactions of the laser circuit, for example, in the ternary
collisions. There are no data on the relaxation constants or similar reac-
tions in the literature. In the case of weak initiation there is optimal
concentration of the photodissociating component leading to the maximum out-
put power (see Figure 1). This optimum with respect to the concentration of
the photodissociating component is probably caused by competition of the in-
crease in the proportion of usefully absorbed light with an increase in pres-
sure of the photodissociating component and an increase in its "extinguish-
ing" effect. However, for the performed measurements it does not appear
possible to find the "light" efficiency, in particular, as a result of a
significant difference in the generation and initiation pulses with respect
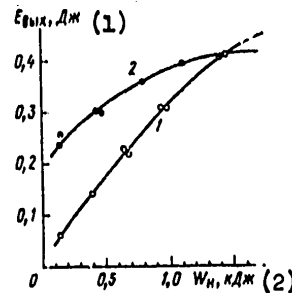to duration and shape.

Figure 4. Output energy of the lasers based on mixtures of 40 ClF + 12 H_2 +
66 He (1) and 40 ClF + 12 H_2 + 62 He + 4 VF_5 (2) as a function of
the initiation energy.

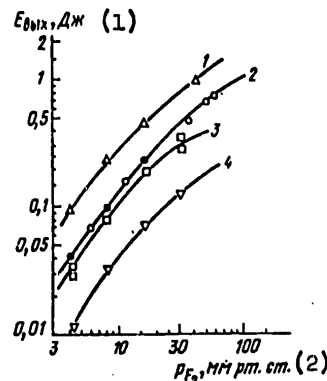Key: 1. E_{out}, joules   2. Kilojoules

Figure 5. Output energy of the lasers based on mixtures of F_2:H_2:MoF_6:He =
1:0.3:0.1:16.6 (2, 3) and 1:0.3:16.7 (1, 4) as a function of the
F_2 pressure for the initiations 1 (3, 4) and 2 (1, 2).

Key: 1. E_{out}, joules   2. mm Hg

70

In addition to the MoF_6 and the VF_5, a study was made of the effect of the ClF_5, WF_6, JF_7 on the generation in mixtures of $ClF-H_2$ and F_2-H_2. The laws of the effect of all of the photoinitiating components are basically identical.

Thus, the effect of the various photoinitiating components on the output power of the investigated chemical lasers indicates that for a comparatively low-power light initiation, and for low pressures of the reactive components (to 50 mm Hg) the efficiency of the lasers can be significantly increased by introducing up to 10 percent of the photoinitiating component. At high pressure of the laser mix and for powerful initiation, the addition of the photoinitiating component can lead to improvement of the output parameters of the lasers.

BIBLIOGRAPHY

1. L. D. Hess, J. APPL. PHYS., No 43, 1972, p 1157.

2. N. G. Basov, S. I. Zavorotnyy, Ye. P. Markin, A. I. Nikitin, A. N. Orayevskiy, B. L. Borovich, P. G. Grigor'yev and V. S. Zuyev, KVANTOVAYA ELEKTRONIKA, No 1, 1974, p 560.

3. D. B. Nichols et al., J. APPL. PHYS., No 47, 1976, p 4026.

4. N. Kh. Petrov, N. F. Chebotarev and S. Ya. Pshezhetskiy, KVANTOVAYA ELEKTRONIKA, No 4, 1977, p 2244.

5. A. N. Chester and L. D. Hess, IEEE J., QE-8, 1972, p 1.

6. Yu. A. Kolchin, V. B. Kolovskiy, S. Ya. Pshezhetskiy and N. F. Chebotarev, KVANTOVAYA ELEKTRONIKA, No 5, 1978, p 2642.

10845
CSO: 8144/0821-22

UDC 621.373.826.038.823

MEASUREMENT OF THE AMPLIFICATION COEFFICIENT IN A SUPERSONIC MIXING JET FOR D-O_3-CO_2

[Article by A. S. Bashkin, A. G. Velikanov, N. M. Gorshunov, Yu. A. Kunin, Yu. P. Neshchimenko, A. N. Orayevskiy and N. N. Yuryshev, Physics Institute imeni P. N. Lebedev of the USSR Academy of Sciences, Moscow; submitted 6 July 1978]

[Text] In [1] a report was made on obtaining generation in a mixture of D-O_3-CO_2 in the continuous (more precisely, quasicontinuous) regime. The experimental device used there was described in [2]. The output generation power obtained amounted to a total of 1.5 watts. However, the radiation power insufficiently completely characterizes the possibilities of the system, for it depends on the length of the amplification region and the quality of the resonator (the transition and reflection coefficients of the mirrors, the quality of the adjustment, and so on).

A more objective index is the amplification coefficient of the radiation determined by the magnitude of the population inversion and characterizing the oscillatory energy reserve in the system. In addition, knowledge of the amplification coefficient permits comparison of the feasibility of various types of CO_2 lasers. Therefore we measured the amplification coefficient of a weak signal in a supersonic mixing jet of atomic deuterium, ozone and carbon dioxide. In view of the short length of the active medium, a three-way measuring circuit was used. The source of the sounding radiation was an LG-23 laser. Special measures were adopted to improve the stability of its output power. The IKS-21 spectrograph was used to monitor the radiation wavelength. The Ge-Au photoresistances were used as the radiation receivers.

First of all the amplification coefficient was measured under the conditions under which generation was obtained in [1]. An oscillogram of the amplification pulse is presented in Figure 1. It is obvious that the signal has the same shape as the generation in [1]. The amplification coefficient under these conditions was 0.2 m^{-1}.
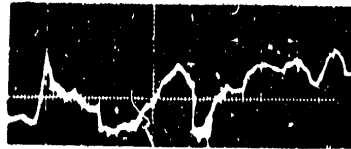
FOR OFFICIAL USE ONLY

Figure 1. Amplification pulse oscillogram.

In order to improve the efficiency of mixing and improve the parameters of the laser a new ejector was used which is analogous to that used in [3]. It had the following distinguishing features by comparison with the old ejector: the ratio of the ejected flow cross section to the ejecting gas cross section was increased; the characteristic diffusion thickness was decreased; the injection point of the gas was brought closer to the critical cross section of the nozzle, as a result of which the relative flow velocity diminished; the single ejector was replaced by an ejector array. All of this led to an increase in the mixing rate and an increase in the uniformity of the flow.
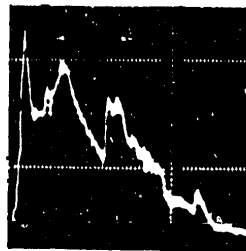

Figure 2. Amplification pulse oscillogram obtained with a new ejector.

More than 50 experiments were performed with the new ejector. The amplification coefficient measured under various conditions is within the range of $0.9-2.1 \text{ m}^{-1}$. An oscillogram of the amplification pulse from the experiment is presented in Figure 2. Amplification of 2.1 m^{-1} was recorded in this experiment. In this case the operating conditions were as follows: initial pressure of the mixture $D_2:Ar = 1:15$ in the low-pressure channel of the shock tube 0.095 atmosphere, speed of the incident shock wave 1.43 km·sec^{-1}, initial pressure of the mixture $O_3:CO_2:He = 1:3:30$ in the valve 3.25 atmospheres.

A measurement was made of the generation power with a new ejector. A resonator was used formed by a blind spherical mirror with a radius of curvature of 3 m and gold coating and a plane output dielectric mirror with transmission coefficient of 6 percent.

FOR OFFICIAL USE ONLY

The maximum recorded power was 36 watts. Optimization of the resonator was not carried out.

The performed studies indicate the prospectiveness of using the reaction of atomic deuterium with ozone as a source of chemical pumping of the CO_2 laser operating in the continuous mode. Therefore the studies of the $D-O_3-CO_2$ system will be continued.

BIBLIOGRAPHY

1. A. S. Bashkin, N. M. Gorshunov, Yu. A. Kunin, Yu. P. Neshchimenko, A. N. Orayevskiy and N. N. Yuryshev, KVANTOVAYA ELEKTRONIKA, No 3, 1976, p 1142.

2. A. S. Bashkin, N. M. Gorshunov, Yu. A. Kunin et al., KVANTOVAYA ELEK-TRONIKA, No 3, 1976, p 462.

3. A. V. Krauklis, V. N. Kroshko, R. I. Soloukhin and N. A. Fomin, FIZIKA GORENIYA I VZRYVA, No 5, 1976, p 792.

10845
CSO: 8144/0821-22

FOR OFFICIAL USE ONLY

UDC 621.375.826

STUDY OF THE ENERGY PARAMETERS OF AN ELECTRON-BEAM-INITIATED ClF-H$_2$ CHEMI-CAL LASER

[Article by A. S. Bashkin, A. F. Konoshenko, A. N. Orayevskiy, S. Ya. Pshezhetskiy, V. N. Tomashov, N. F. Chebotarev and N. N. Yuryshev; submitted 6 July 1978]

[Text] At the present time the chemical laser based on the chain reaction of hydrogen with fluorine has the best energy characteristics. However, the mixture of H$_2$-F$_2$ has a number of deficiencies, the main ones of which are its instability and the presence of a thermal reaction leading to an increase in the initial concentration of the HF molecules strongly deactivating the laser levels. In order to find chemical systems free of the indicated deficiencies, a study was made of the energy parameters of an electron-beam-initiated ClF-H$_2$ chemical laser. The mixture of ClF-H$_2$ is distinguished by much greater stability than H$_2$-F$_2$. In addition, the simultaneous generation on HF molecules (λ_g = 2.7-3.5 microns) and HCl (λ_g = 3.6-4 microns) is an interesting characteristic feature of the ClF-H$_2$ laser. The emission of the HCl molecules is absorbed much more weakly in the atmosphere than the emission of the HF molecules.

Generation on a mixture of ClF-H$_2$ was observed for the first time in [1]. Later, deeper studies were made of the operation of this laser to discover the mechanism of the formation of an inversion and determination of the rate constants of the basic processes [2]. A study was made of the energy characteristics of the ClF-H$_2$ laser with photoinitiation.

Under the conditions of experimentation with photoinitiation the efficiency with respect to the pumping energy absorbed in an active medium was 200 percent as opposed to 500 percent for the H$_2$-F$_2$ laser under analogous conditions. The magnitude of the specific energy output of the ClF-H$_2$ laser is 2.5 times less than the specific energy output of the H$_2$-F$_2$ laser with an identical magnitude of the light energy absorbed in the mixture.

The light efficiency of an H$_2$-F$_2$ laser obtained in experiments with photoinitiation is quite large, but it is essentially inferior to the efficiency

75

FOR OFFICIAL USE ONLY

achieved during electroinitiation which is distinguished by much higher power. Thus, in our experiments values of the efficiency greater than 900 percent have been achieved. It is necessary to consider that the actual difference in efficiency is much greater inasmuch as the energy expenditures on obtaining a fluorine atom during electroinitiation (12 ev [3]) is six times greater than during photoinitiation, that is, the length of the optical circuit in the H_2-F_2 laser with electroinitiation is ~11 times greater than during photoinitiation. In this paper a study was made of mixtures of $ClF-H_2$ using electroinitiation, and a comparison was made between the generation properties of mixtures of H_2-F_2 and $ClF-H_2$ for electroinitiation.

The diagram of the experiment was analogous to the diagram presented in [4]. The electron beam at the input to the couvette had an energy of ~5.6 joules for a current of ~700 amps and an electron energy of ~200 kev. The pulse duration of the electron current is ~40 nanoseconds. The energy of the electron beam absorbed in the working medium of the laser was determined by measuring the energy loss of the electron beam on passage through a gas medium. These measurements were realized using a portable carbon calorimeter placed in the laser couvette. In connection with the high aggressiveness of F_2 and ClF, the working medium of the laser was simulated by sulfur hexafluoride and oxygen. The density of the simulators was selected equal to the density of the working medium. The energy of th(laser emission was measured by the TPI-5A calorimeter, and the duration and shape of the pulse by the FSG-22 photodiode.

The optimal ratio $(H_2/ClF)_{opt}$ was measured initially. The measurements were performed for a ClF pressure of 75 mm Hg. The value of the ratio $(H_2/ClF)_{opt}$ turned out to be 0.4, which differs from the value of $(H_2/ClF)_{opt} = 0.2$ obtained during photoinitiation of a mixture containing the same amount of ClF. In further experiments, mixtures were used with the optimal ratio $(H_2/ClF)_{opt}$.

The measured duration of the generation on the mixture of $ClF:H_2:He = 2.5:1:2.5$ for a pressure of ~225 mm Hg was 1.5 microseconds under these conditions (see Figure 1), which is essentially shorter than for photoinitiation, for which for an analogous mixture the characteristic values were tens of microseconds. This difference is obviously connected with the difference in initiation power.

A comparison of the energy characteristics of the $ClF-H_2$ and the H_2-F_2 lasers was made for mixtures of optimal composition $ClF:H_2:He = 2.5:1:2.5$ and $F_2:O_2:H_2:He = 1:0.08:0.35:5$ [4]. Figure 2 shows the output power of the $ClF-H_2$ laser as a function of the pressure of the mixture. Just as in the case of photoinitiation, the magnitude of the output power of the $ClF-H_2$ laser increases linearly with the pressure of the mixture. For a ClF pressure of 100 mm Hg, the density of the mixture of this composition coincides with the density of the medium of the F_2-H_2 laser containing 100 mm Hg of F_2. In the case of identical densities of the compared mixtures, the electron-beam energy absorbed in them is also identical and equal to ~1 joule. A comparison of this value with the output energies of the H_2-F_2 and the H_2-ClF lasers

76

FOR OFFICIAL USE ONLY

gives efficiencies of 670 and 170 percent, respectively, with respect to the inputed energy. The indicated value of the efficiency of the ClF-H_2 laser remained constant in the pressure range of ClF of 50-150 mm Hg. The beam energy absorbed in the mixture varied from 0.4 to 1.5 joules, and the energy output varied from 6 to 22 joules/liter.
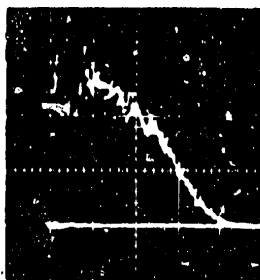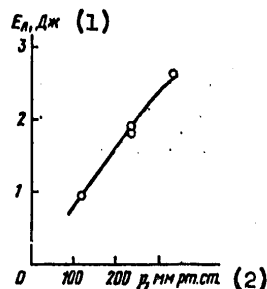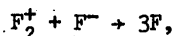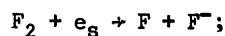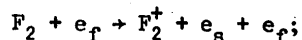

Figure 1. Generation pulse oscillogram.

Figure 2. Output power of the laser as a function of the pressure of a mix-
ture of ClF:H_2:He = 2.5:1:2.5.

Key: 1. Joules   2. mm Hg

As is known, the mechanism of the formation of atomic fluorine in a mixture of F_2-H_2 includes the following processes [3]:

$$F_2 + e_f \rightarrow F_2^+ + e_s + e_f;$$

$$F_2 + e_s \rightarrow F + F^-;$$

$$F_2^+ + F^- \rightarrow 3F,$$

where e_f, e_s are the fast and secondary electrons. Consequently, one act of ionization of an F_2 molecule by fast electron leads to the formation of four F atoms (without consideration of losses). The beam energy expended on the

77

formation of one F atom is in this case ~12 ev [3]. Obviously for the $ClF-H_2$ system it is possible to propose an analogous mechanism:

$$ClF + e_f \rightarrow ClF^+ + e_f + e_s;$$

$$ClF + e_s \rightarrow Cl^- + F;$$

$$Cl^- + ClF^+ \rightarrow 2Cl + F.$$
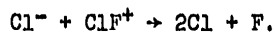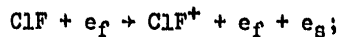
The Cl atoms formed as a result of the ion reactions also can yield F atoms in the reaction of $Cl + ClF \rightarrow Cl_2 + F$ ($K = 0.54 \cdot 10^{-12}$ cm^3/sec). The time constant of this process under the experimental conditions is ~600 nanoseconds, which is essentially shorter than the generation duration. Taking this process into account, the expenditures on the formation of one F atom will be, just as in the H_2-F_2 laser, equal to ~12 ev. Therefore it is possible to draw the conclusion that: under the conditions of the performed experiments the proportion of the laser energy for one F atom in the H_2-F_2 system is four times greater than in the $ClF-H_2$ system. The energy contained in the emission of the HCl molecules was measured. For this purpose the integral emission of the laser was separated by a prism, and a diaphragm which cut off the emission of the HF molecules was placed at the focal plane of the collecting spherical mirror located outside the prism. It turned out that the generation energy on HCl is 24 percent of the total output energy of the laser. Thus, the efficiency of the $ClF-H_2$ HCl laser is ~40 percent with respect to the energy absorbed by the mixture.

As is obvious from Figure 2, the magnitude of the maximum laser energy obtained on a mixture of $ClF-H_2$ is 2.6 joules. The proportion of the HCl generation is 0.62 joule which corresponds to an average generation power of 0.4 megawatts for an energy output of 5 joules/liter. The presented values are obviously record values for HCl lasers. Therefore the $ClF-H_2$ HCl laser can be highly prospective under conditions where it is necessary to obtain coherent radiation with a frequency corresponding to the transitions of the HCl molecule, for example, for purposes of laser chemistry.

BIBLIOGRAPHY

1. O. D. Krogh and G. G. Pimentel, J. CHEM. PHYS., No 56, 1972, p 969.

2. N. F. Chebotarev, candidate's dissertation, NIKhFI, Moscow, 1978.

3. J. Wilson, H. L. Chen, W. Fyfe, R. L. Taylor, R. Little and R. Lowell, J. APPL. PHYS., No 44, 1973, p 5447.

4. A. S. Bashkin, A. F. Konoshenko, A. N. Orayevskiy, V. N. Tomashov and N. N. Yuryshev, KVANTOVAYA ELEKTRONIKA, No 5, 1978, p 1608.

10845
CSO: 8144/0821-22

FOR OFFICIAL USE ONLY

EFFECT OF GROUP VELOCITY MISMATCH ON THE REPRODUCTION OF THE PUMPING SPEC-
TRUM IN THE CASE OF STIMULATED SCATTERING

[Article by B. Ya. Zel'dovich and V. V. Shkunov, Physics Institute imeni
P. N. Lebedev of the USSR Academy of Sciences, Moscow; submitted 5 July
1978]

[Text] The problem of the reproduction of the spatial [1, 2] and time [3,
4] structures of the pumping field by the scattered wave field in the case
of stimulated scattering of light has been discussed with great interest in
recent times. The mechanism of the reproduction of a spatial
structure consists in a primary (two times larger) amplification coefficient
of the scattered wave configuration for which the interference peaks coin-
cide with the pumping peaks in the entire interaction volume in spite of
diffraction. Let us emphasize that multiple alternation of the peaks and
the minima as a result of diffraction "is tied onto" the reproducing struc-
ture. For forward scattering we have the ratio $E_S(r) \sim E_L(r)$, and for back-
scattering $E_S(r) \sim E_L^*(r)$. A qualitatively different physical cause provides
the basis for reproduction of the time structure [4]. In the case of a non-
monochromatic pumping field $E_L(t)$ under defined conditions it is possible to
achieve highly effective (resonance) buildup of the molecular vibrations if
the scattered wave $E_S(t)$ has the form $E_S(t) = \mathrm{const} \cdot e^{i(\omega_L - \omega_S)t} E_L(t)$ (let us empha-
size that in the time problem of forward scattering and backscattering we are
talking about reproduction without complex conjugation). Indeed, in this
case the force $F(t) \sim e^{i(\omega_L - \omega_S)t} |E_L(t)|^2$ building up the disturbances of the medium
contains a monochromatic component proportional to the mean $|E_L(t)|^2$ with re-
spect to time, and the scattering of the laser field $E_L(t)$ on the monochro-
matic disturbances of the medium gives the reproduction of the time struc-
ture $E_S(t) \sim E_L(t) e^{i(\omega_L - \omega_S)t}$.

In spite of the difference in physical mechanisms of reproduction of the
space and time structures, their mathematical description in terms of the
angular and frequency spectra, respectively, under the defined conditions
(see [3]) leads to similar equations. This paper is devoted to considera-
tion of the effect of the mismatching of the group velocities of the pumping
and the scattered wave on the reproduction of the time structure in the case

79
FOR OFFICIAL USE ONLY

of stimulated scattering. The mathematical methods developed earlier [2] for the problem of reproduction of the spatial structure in the presence of stimulated Raman scattering are used in the investigation.

The equations of the theory of the nonstationary stimulated scattering of plane waves [3-5] will be written in the form

$$\frac{1}{u_L}\frac{\partial E_L}{\partial t} \pm \frac{\partial E_L}{\partial z} = 0; \quad \frac{1}{u_s}\frac{\partial E_s}{\partial t} + \frac{\partial E_s}{\partial z} = \gamma_s \sigma E_L; \quad \frac{\partial \sigma}{\partial t} + \frac{1}{\tau}\sigma = \gamma_\sigma E_L^* E_s, \tag{1}$$

where the "+" and "-" signs in the first equation describe the stimulated forward scattering and backscattering, respectively; σ is the slow amplitude of the vibrations of the medium.

The solution of the equation for the pumping field will be represented in the form of an expansion with respect to spectral components with frequencies Ω reckoned from some central frequency ω_{L0}

$$E_L(z, t) = E_L\left(t \mp \frac{z}{u_L}\right) = \sum_\Omega C(\Omega)\exp\left\{-i\Omega\left(t \pm \frac{z}{u_L}\right)\right\}. \tag{2}$$

Inasmuch as we are interested in the problem of the reproduction of the time structure, we shall find the solution for the scattered wave in the form of an expansion with respect to the same spectral components:

$$E_S(z, t) = \sum_\Omega S(\Omega, z)\exp\left\{-i\Omega\left(t \mp \frac{z}{u_L}\right)\right\}. \tag{3}$$

Let us emphasize that in contrast to [3], the structure matched in the plane (z, t) with the pumping field structure is tied onto the scattered wave field in spite of the difference in group velocities. For a sufficiently great distance between the spectral components $|\Omega_i - \Omega_{i+1}|\tau \geq 1$, we obtain the equation

$$\frac{\partial S(\Omega, z)}{\partial z} - i\frac{\Omega}{u_L}\alpha S(\Omega, z) = \frac{1}{2}GC(\Omega)\sum_\Omega C^*(\Omega)S(\Omega, z), \tag{4}$$

where $\alpha = (u_L \mp u_S)/u_S$ ($\alpha = v/u_L$ in the notation from [3]); $G = 2\gamma_S\gamma_\sigma\tau$ is the characteristic of the steady-state amplification coefficient of the medium; $g[cm^{-1}] = G|E_L|^2$.

System (4) permits the search for the solution in the form $S(\Omega, z) = \exp\{\mu z\}S(\Omega)$. Then this solution has the following form:

$$S(\Omega) = \frac{1}{2}GD\left[\mu - i\alpha\frac{\Omega}{u_L}\right]^{-1}C(\Omega); \quad D = \sum_\Omega C^*(\Omega)S(\Omega). \tag{5}$$

The equation for the eigenvalues of the amplitude increment has the form

$$l = \frac{1}{2} G \sum_{\Omega} |C(\Omega)|^2 \left[\mu - i\pi \frac{\Omega}{u_L} \right]^{-1}.$$ (6)

As is known [2, 3], for small effect of the mismatch there is a reproducing solution of the system of the type of (5), (6) of the form $S(\Omega) = \text{const} \cdot C(\Omega)$ with the increment $\mu = 0.5$ GI, where $I = \Sigma |C(\Omega)|^2$ is the mean pumping intensity with respect to time. In addition, for system (5), (6) there are a number of nonreproducing solutions which have a zero increment in the investigated approximation. (Let us note that the difference in physical mechanisms of reproduction of the time and space structures is felt here.)

Considering the mismatch of the group velocities, the reproducing solution assumes the form (5) with the value of μ equal to

$$\mu = \frac{1}{2} GI + i \frac{\alpha}{u_L} \langle \Omega \rangle - \frac{2\alpha^2}{GI} \frac{\langle \Omega^2 \rangle - \langle \Omega \rangle^2}{u_L^2}.$$ (7)

Here we arrive at the expression for μ with accuracy to the terms $\sim(\alpha\delta\Omega)^2$, inclusively; the angular brackets indicate averaging with respect to the frequency pumping spectrum. The time behavior of this solution corresponds to reproduction with smoothing:

$$E_S(z, t) = \int_{-\infty}^{+\infty} E_L(z, t') F(t - t') dt',$$ (8a)

where $F(\tau)$ is the Fourier transform of the spectral function of the transfer from (5):

$$F(\tau) = \text{const}\,\theta(\tau) \exp\left\{ -\frac{\mu u_L}{\alpha} \tau \right\}.$$ (8b)

For $\alpha \to 0$ the reproduction becomes exact. The inaccuracy of reproduction for $\alpha \neq 0$ leads to a decrease in the increment by the amount

$$|\Delta g| = -2\text{Re}\Delta\mu = g_0 4 \frac{\alpha^2}{(GI)^2} \frac{\langle \Omega^2 \rangle - \langle \Omega \rangle^2}{u_L^2},$$ (9)

where $g_0 = GI$ is the amplification coefficient for exact reproduction (coinciding with the steady-state value). Let us note that expression (9) does not depend on the selection of the central frequency from which the spectral tuning out Ω is reckoned.

The nonreproducing modes approximately correspond to the excitation of individual spectral components of $C(\Omega)$ in the scattered wave and the corresponding eigenvalue of μ turns out to be almost purely imaginary: $\mu_\Omega \approx i\Omega\alpha/u_L$ and it describes the propagation of the scattered wave with its own velocity u_S.

81

FOR OFFICIAL USE ONLY

It is clear that the group mismatch leads to disruption of the reproduction of the time structure for $|\Delta g|/g_0 = 1$. Formulas (8), (9) of this paper permit formulation of the reproduction criterion (with respect to the group mismatch effects) quantitatively, expressing it in terms of the parameters $\langle \Omega \rangle$ and σ. $\langle \Omega^2 \rangle - \langle \Omega \rangle^2$ in the mean value and the dispersion of the frequency in the pumping spectrum.

Let us consider the extraordinary properties of the reproducing mode in the case of the greatest mismatch of the group velocities: in the case of back-scattering ($\alpha \approx 2$). For $\Delta g/g_0 \lesssim 1$ the wave mode $E_S(z, t)$ has the form

$$E_S(z, t)\, e^{-i\omega_S t + i k_S z} \approx E_L\left(t + \frac{z}{u_L}\right) e^{-i\omega_S t + i k_S z}. \tag{10}$$

In other words, the envelope for this mode goes matched with the pumping in the direction of $-z$ with a velocity $u = u_L$ although the phase velocity and the energy flux are in the $+z$ direction. The fact that the group wave velocity can vary by many times in media with significantly nonstationary gain has already been noted (see, for example, [6]). Let us illustrate this within the framework of the system of equations (1). We shall consider the pumping monochromatic and constant in the entire volume, and we shall consider the amplification of the input Stokes pulse. Assuming the value of τ to be a small parameter, the last of the equations (1) for $E_L = \text{const}$ can be solved by the iteration method:

$$\sigma = \gamma_\sigma \tau E_L^* E_S - \gamma_\sigma \tau^2 E_L^* \frac{\partial E_S}{\partial t} + \gamma_\sigma \tau^3 E_L^* \frac{\partial^2 E_S}{\partial t^2} + \cdots \tag{11}$$

Substitution of this solution in the second of the equations (1) gives

$$\frac{\partial E_S}{\partial z} + \frac{\partial E_S}{\partial t}\left(\frac{1}{u_S} + \frac{g\tau}{2}\right) = \frac{g}{2} E_S + \frac{g}{2}\tau^2 \frac{\partial^2 E_S}{\partial t^2} + \cdots \tag{12}$$

Thus, the part of the Stokes wave which is amplified with the gain g [cm^{-1}] (with respect to intensity) will receive a positive addition of the $g\tau/2$ to the magnitude of the inverse group velocity u^{-1}. For $g\tau \gg u_S^{-1}$ this indicates a decrease in the group velocity by many times. The time for passage through a medium of length L with this (decreased) group velocity $t \approx (gL/2)\tau$ coincides [6] with the time of establishment of the stimulated scattering mode with a stationary gain g.

In these terms for the nonstationary pumping $E_L(t + z/u_L)$ part of the scattered field (reproducing mode) can have a group velocity differing from the initial one even in the same sign.

82

FOR OFFICIAL USE ONLY

FOR OFFICIAL USE ONLY

BIBLIOGRAPHY

1. B. Ya. Zel'dovich, V. I. Popovichev, V. V. Ragul'skiy and F. S. Fayzul-
   lov, PIS'MA V ZhETF, No 15, 1972, p 160; B. Ya. Zel'dovich, N. A. Mel'-
   nikov, N. F. Pilipetskiy and V. V. Ragul'skiy, PIS'MA V ZhETF, No 25,
   1977, p 41.

2. B. Ya. Zel'dovich and V. V. Shkunov, KVANTOVAYA ELEKTRONIKA, No 4, 1977,
   p 1090.

3. G. P. Dzhotyan, Yu. Ye. D'yakov, I. G. Zubarev, A. B. Mironov and S. I.
   Mikhaylov, KVANTOVAYA ELEKTRONIKA, No 4, 1977, p 1377; V. G. Sidorovich,
   KVANTOVAYA ELEKTRONIKA, No 5, 1978, p 1356.

4. C. S. Wang, PHYS. REV., No 182, 1969, p 481; Yu. Ye. D'yakov, PIS'MA
   V ZhETF, No 9, 1969, p 487.

5. I. M. Bel'dyugin, Ye. M. Zemskov and V. I. Chernen'kiy, KVANTOVAYA ELEK-
   TRONIKA, No 5, 1978, p 1349.

6. B. Ya. Zel'dovich, PIS'MA V ZhETF, No 15, 1972, p 226.

10845
CSO: 8144/0822   END

FOR OFFICIAL USE ONLY